

Confinement effects on diffusiophoretic self-propellers

M. N. Popescu*

Ian Wark Research Institute, University of South Australia, 5095 Adelaide, South Australia, Australia

S. Dietrich[†]

*Max-Planck-Institut für Metallforschung, Heisenbergstr. 3, 70569 Stuttgart, Germany, and
Institut für Theoretische und Angewandte Physik,
Universität Stuttgart, Pfaffenwaldring 57, 70569 Stuttgart, Germany*

G. Oshanin[‡]

*Laboratoire de Physique Théorique de la Matière Condensée,
Université Pierre et Marie Curie (Paris 6) - 4 Place Jussieu, 75252 Paris, France*

(Dated: February 3, 2022)

We study theoretically the effects of spatial confinement on the phoretic motion of a dissolved particle driven by composition gradients generated by chemical reactions of its solvent, which are active only on certain parts of the particle surface. We show that the presence of confining walls increases in a similar way both the composition gradients and the viscous friction, and the overall result of these competing effects is an increase in the phoretic velocity of the particle. For the case of steric repulsion only between the particle and the product molecules of the chemical reactions, the absolute value of the velocity remains nonetheless rather small.

PACS numbers: 89.20.-a, 07.10.Cm, 82.56.Lz

1. INTRODUCTION

Recent years have witnessed a growing technological, experimental, and theoretical interest in scaling standard machinery down to micro- and nano-scales as needed for the development of “lab on a chip” devices. For applications in, e.g., drug-delivery systems or micromechanics one of the most challenging problems at this stage is to develop ways to enable small-scale objects to perform autonomous, controlled motion^{1,2}. Although the research in this area is still in its early stages, several such proposals have already been tested experimentally (see, e.g., Refs. 3,4,5,6). A review of the recent progress in this field can be found in Ref. 2.

Whitesides and co-workers proposed a design of self-propelling devices based on an asymmetric decoration of the surface of small objects by catalytic, active sites promoting a chemical reaction in the surrounding liquid medium³. This asymmetric distribution can provide motility through a variety of mechanisms, such as surface tension gradients and/or cyclic adsorption and desorption^{2,7}. The use of an asymmetric surface distribution of a catalyst has been further proposed for an autonomous diffusiophoretic motion emerging as a result of self-created density gradients⁵. An experimental realization of such systems, using platinum coated polystyrene spheres, has been recently reported⁶. The issue of designing optimal distributions of a catalyst for spherical and rod-like particles has also been approached⁸.

For most of the applications in biological systems or in ‘lab on a chip’-type devices one has to deal with a complicated internal structure of the systems, such as networks of narrow channels or pores and various impenetrable impurities. In some situations, one may even encounter

a quasi two- or one-dimensional behavior, like in the cases of bacteria motion on planar nutrient substrates⁹ and of the motion of small particles within a biological membrane¹⁰ or in a monolayer adsorbed on a three-dimensional ($3d$) liquid subphase¹¹. Thus spatial confinement is a relevant feature so that the assumption of the presence of an unconfined $3d$ bulk reactive solvent^{1,2,5} may break down. Intuitively, one expects that spatial confinement does influence the resulting motion of self-propelling objects like the ones discussed above. But *a priori* it is not clear if such effects are significant.

Starting from the model used in Ref. 5, here we study the effects of spatial confinement on the phoretic motion of a particle that generates number density gradients of the product molecules emerging from the chemical reactions in the depleting Newtonian liquid solvent. We shall focus on the simple case in which the particle and the $3d$ solution of solvent and product molecules are bounded by a spherical shell because (i) this simple geometry allows for an exact solution and (ii) it has been experimentally shown for a variety of phoretic systems that confinement effects are dominated by the smallest confining length scale¹². Thus this geometry has a paradigmatic character.

Similarly to the earlier studies^{1,2,4,5,6}, our work is based on adopting the standard theory of phoresis for the present case, in which the gradients are self-generated rather than being produced and maintained by external sources. In doing so, one is bound to make a number of assumptions that are either already present in the classical theory of phoresis, or arise as a result of mapping the description of such “active” surface particles onto the framework of a theory developed to describe the case of inert particles immersed in a pre-defined, externally

controlled concentration gradient. Since in the literature these assumptions are often overlooked or not spelled out explicitly, we consider it as necessary to provide also a critical discussion of the significant assumptions involved by this mapping, as well as of some of those assumptions implicitly contained in the standard theory of phoresis. Accordingly, the outline of this paper is as follows. In Section 2 we define the model and discuss some general aspects of systems with self-generated motion, with particular emphasis on the assumptions involved in adopting the standard theory of phoresis. Section 3 is devoted to the computation of the diffusiophoretic velocity. This includes the calculation of the diffusiophoretic slip velocity and the determination of the phoretic hydrodynamic flows and density profiles of the product molecules around a self-propelling particle. The results are discussed in Section 4, and we conclude in Section 5 with a brief summary of our results and general conclusions. Important details of our calculations are presented in the Appendices A, B, and C.

2. THE MODEL

2.1. General aspects.

The system we consider is shown in Fig. 1. It consists of an impermeable, spherical particle of radius R with a point-like catalytic site (black dot in Fig. 1) on its surface, which promotes the chemical conversion of a surrounding solvent into product molecules of diameter a (small hatched circles in Fig. 1). The particle and the surrounding solution (solvent plus the solute, i.e., the product molecules) of viscosity μ are enclosed in a concentric, impermeable, spherical shell of radius $R_1 = \eta R$ ($\eta > 1$).

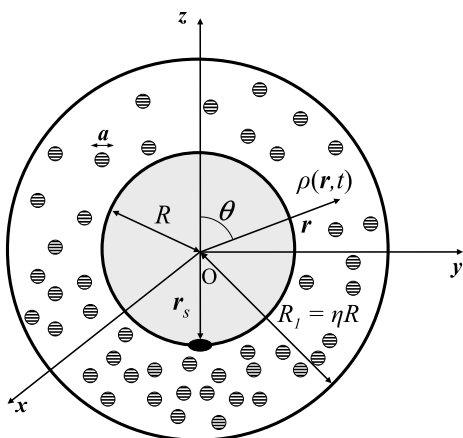


FIG. 1: An impermeable, spherical particle of radius R with a point-like catalytic site at $\mathbf{r}_s = -R\mathbf{e}_z$ (depicted as a black dot) on its surface, enclosed by a concentric, impermeable, spherical wall of radius $R_1 = \eta R$ ($\eta > 1$). The product molecules of diameter a are shown as small horizontally hatched circles.

In general, such a chemical conversion of the solvent gives rise to several types of product molecules. Here we shall focus on the particular case in which the chemical conversion of a solvent molecule (A) leads to two molecules only (A' and B), one very similar in size and properties with the solvent itself ($A' \approx A$), the other one (B) different [$A \xrightarrow{cat} A' + B$]; in the following this latter is denoted as “product molecule” and plays the role of a solute in the solvent. In other words, we consider a situation in which the net result of the chemical conversion can be approximated as the generation of a solute, solely, and the reaction does not lead to a solvent depletion near the catalytic site which otherwise would reduce the current of solvent towards the catalytic site acting as a solvent sink. For example, this is approximately the case for the Pt catalyzed decomposition of hydrogen peroxide (H_2O_2) in aqueous solution into water (H_2O) and oxygen (O_2) molecules, as discussed in Refs. 1,2,6. In these experimental studies the oxygen plays the role of the product molecule the properties of which differ significantly from those of the solvent. Here the solvent is actually a binary liquid mixture of H_2O and H_2O_2 for which H_2O is passive and does not participate in the chemical conversion. We note that actually it is rather difficult to assess whether or not H_2O and H_2O_2 can be treated as being the same in such systems, and probably the answer would be on a case by case basis. This is not only because the H_2O -particle and H_2O_2 -particle interactions may be quite different for different materials (the simplest example is exactly the catalytic decomposition of H_2O_2 on Pt), but also because of the sensitivity of phoresis to the details of the *solvent mediated* interactions – and the weakly acidic nature of H_2O_2 may play an important role here. In providing this example as a possible realization of a catalyzed reaction $A \xrightarrow{cat} A + B$ we had to rely on: (i) the statement in Ref. 2 [second entry, bottom of left column on page 13427 therein], which is based on some previously published results by Phibbs and Giguère¹³, that hydrogen peroxide and water in contact with Au have almost identical interfacial tensions (this translates into similar particle-solvent interactions), and thus that there is no additional solvent-density gradient to be considered, and (ii) on the implicit statement in the same Ref. 2 [second entry, Eq. (8) therein] that the effective interaction of the O_2 molecule with the Au surface of the rod does not depend on the composition of the solvent $\text{H}_2\text{O} - \text{H}_2\text{O}_2$ mixture.

We thus assume that the reaction at the catalytic site, (located at $\mathbf{r}_s = -R\mathbf{e}_z$, where \mathbf{e}_z is the unit vector of the z -axis), acts effectively only as a point-like source of product molecules⁵ of diameter a which are diffusing in the solvent with diffusion coefficient D . In passing we note that this is in contrast to the situation considered in Ref. 7, where the catalytic site acts both as a source for the product and as a sink for the solvent, i.e., the generation of a product molecule is accompanied by the annihilation of a solvent one so that $A \xrightarrow{cat} B$ which implies that B can

only be a different configuration of A , because it must have the same chemical constituents. In the situation considered here, the amplitude of the production rate of B is denoted as $B(t)$. We shall neglect any interaction between the product molecules. Thus the number density of product molecules is considered to be so low that among themselves they behave like an ideal gas. There is an interaction potential between the product molecules and the moving particle (see Appendix A), which includes the impermeability condition at the surface of particle. The interactions between the product molecules and the solvent are accounted for in an effective way via the Stokes - Einstein expression $D = k_B T / (3\pi\mu a)$ for the diffusion coefficient D of the product molecules¹⁴, where k_B is the Boltzmann constant and T is the temperature.

2.2. Discussion of the model in the context of the standard theory of phoresis.

The presence of a source of solute (product molecules) on the surface of the particle creates a non-uniform and time dependent distribution of solute in the solution (see Fig. 1), i.e., a non-uniform composition of the solution. Because the understanding of the way in which such a non-uniform composition gives rise to phoretic motion is not straightforward, we discuss here in some detail how the general model introduced in Section 2.1 can be put into the context of the standard theory of phoresis¹². A recent clear exposition of the basic concepts and a discussion of different phoretic transport scenarios can be also found in Ref. 15.

If the production rate of the source is not very large and the diffusion coefficient of the product molecules through the solvent is not too small, the solute density varies smoothly in space and slowly in time. This justifies the assumption of local equilibrium and the definition of a position- and time-dependent chemical potential of the solution (the spatial gradients of which describe the diffusion of the solute away from the source). In a quasi steady-state of the solution, corresponding to slow time-variations of the composition, the net solute current is approximately zero and the solute density gradients are balanced by pressure gradients [see also Eq. (B3) in Ref. 15]. Because in the absence of external body forces the mechanical equilibrium for a liquid solution is generally established much faster than the chemical one (see, e.g., Ref. 16), it is physically plausible to assume that *far from the boundaries* (i.e., far from the wall and far from the particle surface) the pressure adjusts instantaneously to accommodate the spatially varying solute density profile¹⁵ and keeps varying slowly with time (on time scales much larger than the diffusion time $\sim R^2/D$) because the overall density of the solution increases in time. In other words, the pressure is determined by the solute density profile and is obtained from the equation of state of the solvent-solute binary mixture considered as a thermodynamic system in local equilibrium described

by the corresponding free energy density. Clearly, the situation is different in the region of contact between the solution and the particle surface (and also of contact with the wall) where the interactions of the particle with the product molecules (solute) and with the solvent molecules are relevant. This interaction disturbs the distribution of solute molecules, net currents of solute and solvent result, and the pressure field becomes a quantity determined by the incompressibility requirement for the hydrodynamic flow, and not by an equation of state. We shall discuss this important point below.

At a given time the spatial variations of the number density ρ of the solute and of the number density ρ_{solv} of the solvent are characterized as follows: ρ_{solv} is constant throughout the solution apart from the close vicinity of the particle surface and of the surface of the confining sphere. There ρ_{solv} vanishes and reaches its constant bulk value via density oscillations which are induced by local packing effects caused by the finite diameter a_{solv} of the solvent particles. Away from any kind of surface phase transition the approach of the bulk value occurs exponentially on the scale of the bulk correlation length ξ_{solv} of the solvent. (The presence of long-ranged dispersion forces causes power-law decays; however, their amplitude is small and is neglected in the present context.) Away from bulk phase transitions ξ_{solv} is comparable with the range of the interaction potential between the solvent molecules, which in turn is proportional to a_{solv} with a prefactor of order unity. Within this picture ρ_{solv} does not vary along the surface of the particle.

The solute number density ρ is characterized by two important features. On the scale of the system size $R \gg a$, ρ varies due to the diffusion process. On the much smaller length scale of the solute diameter a , ρ also varies near the particle surface and near the surface of the confinement as discussed above for the solvent. Since, however, according to our earlier assumption the solute particles can be considered to form an ideal gas, near the walls ρ varies proportional to $\exp(-\beta\Psi)$, where Ψ is the *effective* substrate potential (see Appendix A) in the sense that it describes the interaction of the solute molecule with the substrate in the presence of the solvent, and $\beta = 1/k_B T$. Typically the range δ of Ψ is proportional to the solute diameter a . Accordingly the solute molecules interact directly with the particle only if they are within a thin surface film of thickness δ , which is assumed to not be deformed by the motion of the particle¹².

The standard theory of phoresis assumes $a, \delta \gg a_{solv}$ so that within this surface film of thickness δ the solvent can be considered as a continuum with constant ρ_{solv} . We note that this assumption is rather convenient from a computational point of view. However, this assumption is at odds with the basic underlying model according to which the solute particle is created from a solvent particle via a catalytic reaction. Under these circumstances one expects $a \approx a_{solv}$ (see the above example of the reaction $2 \text{H}_2\text{O}_2 \xrightarrow{cat} 2 \text{H}_2\text{O} + \text{O}_2$). In the absence of a more

detailed theory of phoresis, which treats the sizes of the solvent and solute particles on the same footing, we proceed along the lines of the standard theory. Nonetheless we point out that there is an urgent need for improvement. It might be that due to the fact that continuum hydrodynamics remains quantitatively reliable down to surprisingly small length scales (here a_{solv}), it is conceivable that the aforementioned continuum description yields reliable results, too. But this remains unproven.

According to the standard theory a hydrodynamic description applies within the aforementioned surface film. Within this picture the solute molecules and their effective interaction with the particle are replaced by a corresponding distribution of “point forces” acting on the solvent in the film. Within the limitations of such an approach the hydrodynamic description of the solution naturally splits into that of an “inner” region formed by the surface film and that of the “outer” region formed by the exterior space beyond the surface film. Following Refs. 8,12,17, the ensuing asymmetric, non-uniform solute number density $\rho(\mathbf{r}, t)$ around the particle will give rise, *within the surface film only*, to a pressure gradient along the surface of the particle. This is because the surface film is very thin on the scale of the system size R so that the equilibration of the composition profile of the solution within the surface film can be assumed to be fast along the direction normal to the surface of the self-propelling particle compared with the diffusional relaxation time of the composition gradient along its surface, which typically involves a length scale of the order of the particle size R . Therefore, within the surface film the solute density in the direction normal to the surface of the particle is given by a Boltzmann distribution corresponding to the local equilibrium configuration in the presence of the effective interaction potential between the particle and the solute molecules, with a prefactor which depends on the position along the surface of the particle (for details see Appendix A, which builds on Ref. 12). Mechanical equilibrium of the solvent within the surface film along the direction normal to the surface of the particle (no flow along this direction) requires the pressure gradient along the normal to be equal to the body force densities due to the effective particle-solute interactions. Therefore the pressure within the surface film differs from the “outer” pressure field by an “osmotic pressure” term, i.e., a term proportional to the extra solute density ρ in excess to the constant solvent density ρ_{solv} . Since this osmotic pressure varies along the surface of the particle, there is a gradient of pressure along the surface of the particle. This lateral pressure gradient is not balanced by any body force and thus generates shear stress within the surface film. Therefore it induces hydrodynamic flow of the solution along the surface of the particle and entails motion of the particle with a velocity $\mathbf{V}(t)$. Because the system has azimuthal symmetry, the motion is along the z -axis, i.e., $\mathbf{V} = V\mathbf{e}_z$. The hydrodynamic flow of the solution, the diffusive transport of the solute, and the coupling between the two giving rise to phoretic motion

of the particle are analyzed in detail in the next section (see also the Appendices A-C).

3. COMPUTATION OF THE DIFFUSIO-PHORETIC VELOCITY

Our calculation of the diffusiophoretic velocity proceeds along the lines of Ref. 12 and is based on dividing the problem into an inner one – within the film around the particle surface discussed in Subsec. 2.2, and an outer one – beyond the range of the effective interaction between the solutes and the particle. In view of the arguments presented in Sec. 2, we base our analysis on the following assumptions:

- (i) The chemical reaction leads to a change in the solute density only. The thickness of the surface film, defined by the range of the effective interaction between the product molecules (solute) and the particle, is much smaller than the particle radius R . The spatial variations of the solute number density along the surface of the particle occur over length scales of the order of R , which allows one to use the approximation of a locally planar interface.
- (ii) The number density of product molecules is sufficiently low, so that the solute can be viewed as an ideal gas and the solvent-solute mixture behaves like an ideal dilute solution. In this case, the pressure gradient is simply proportional to the gradient of the number density of the product particles (see Appendix A).
- (iii) Temporal variations of the number density of the product molecules due to their creation occur on time scales much longer than those needed for the fluid flow (as seen from the moving particle) to relax to a steady state corresponding to the number density profile at that moment.
- (iv) The flow field of the solution within the surface film can be described by the laws of hydrodynamics.

Additionally, we assume that both the Reynolds number $\text{Re} \simeq \tilde{\rho}_{solv}VR/\mu$, where $\tilde{\rho}_{solv}$ is the *mass density* of the solvent, and the Peclet number $\text{Pe} \simeq VR/D$ are small, such that one can approximate the hydrodynamic description with the creeping flow (Stokes) equations and disregard the convection of the solute compared to its diffusive transport. Here we have assumed that the magnitude of the hydrodynamic flow \mathbf{u} is similar to that of the phoretic velocity V ; this assumption is supported *a posteriori* by the fact that for our system the phoretic velocity is basically the average of the slip-velocity over the surface of the particle [see, c.f., Eqs. (1) and (10)]. For a μm size particle moving through water (density $\tilde{\rho}_{solv} = 10^3 \text{ kg/m}^3$, viscosity $\mu = 10^{-3} \text{ Pa s}$) with a velocity of the order of $\mu\text{m/s}$, which is typical for phoresis, one has $\text{Re} \simeq 10^{-6}$. For the diffusion at room temperature ($k_B T_{room} \sim 4 \times 10^{-21} \text{ J}$) of O_2 ($a \sim 10^{-10} \text{ m}$) in H_2O_2 ($\mu \simeq 10^{-3} \text{ Pa s}$), the Stokes-Einstein relation leads to an estimate $D \sim 4 \times 10^{-9} \text{ m}^2/\text{s}$ for the diffusion coefficient (in agreement with Ref. 2), and thus $\text{Pe} \simeq 10^{-3}$.

Therefore the latter assumptions are justified. Note that if one uses R_1 rather than R as a characteristic length scale, the above results imply that the Re and Pe numbers remain both very small as long as $\eta \lesssim 10$.

3.1. Diffusiophoretic slip-velocity

As discussed in Sec. 2, the pressure gradient along the surface of the particle, induced by its interaction with the non-uniform distribution $\rho(\mathbf{r}, t)$ of product molecules, leads to flow of the solution relative to the particle. As shown in Appendix A, the hydrodynamic flow within the surface film translates into a (phoretic) slip-velocity,

$$\mathbf{v}_s(\mathbf{r}, t) = -b\nabla_s \rho(\mathbf{r}, t), \text{ for } |\mathbf{r}| = R_+, \quad (1)$$

at the outer edge $R_+ \gtrsim R$ of the surface film as a boundary condition for the hydrodynamic flow in the outer region. In this equation ∇_s denotes the projection of the gradient operator onto the tangential planes of the surface of the particle,

$$\nabla_s = \mathbf{e}_\theta \frac{1}{r} \frac{\partial}{\partial \theta} + \mathbf{e}_\phi \frac{1}{r \sin \theta} \frac{\partial}{\partial \phi}, \quad (2)$$

where \mathbf{e}_θ and \mathbf{e}_ϕ are the polar and azimuthal unit vectors, respectively, while

$$b = \frac{k_B T}{\mu} \Lambda \quad (3)$$

is an effective ‘‘mobility’’, and $\lambda = \sqrt{|\Lambda|}$ is a characteristic length scale. The latter is determined by the effective interaction potential Ψ between the particle and the product molecules¹² [which determines their distribution within the surface film along the direction \hat{y} normal to the particle surface within the local coordinate system (Fig. 3) or the radial direction here]:

$$\Lambda = \int_0^\infty d\hat{y} \hat{y} \left(e^{-\beta\Psi(\hat{y})} - 1 \right). \quad (4)$$

In the case of a purely steric repulsive interaction, one has¹² $\Lambda = -a^2/8$ so that $\lambda = a/(2\sqrt{2})$. For a single catalytically active site as shown in Fig. 1 ρ and thus \mathbf{v}_s do not depend on the azimuthal angle ϕ .

3.2. Phoretic hydrodynamic flow

We focus here on the quasi-static approximation (iii) described above and the limit of low Re numbers. In the laboratory frame, in which the particle moves with a yet unknown velocity $\mathbf{V}(t; \eta)$, the hydrodynamic flow $\mathbf{u} \equiv \mathbf{u}(\mathbf{r}; t, \eta)$ at time t in the domain beyond the surface film around the particle obeys the steady-state force-free

Stokes equations

$$\nabla \cdot \hat{\Pi} = 0, \quad \nabla \cdot \mathbf{u} = 0, \quad R_+ < |\mathbf{r}| < R_1, \quad (5)$$

where $\hat{\Pi} = -p\hat{\mathbf{I}} + \mu\hat{\Sigma}$ is the pressure tensor, p is the hydrostatic pressure, and $\hat{\Sigma}$ is the shear stress tensor, i.e., $\Sigma_{\alpha\beta} = \partial u_\alpha / \partial x_\beta + \partial u_\beta / \partial x_\alpha$, subject to boundary conditions (BC) of no-slip at the wall at R_1 and prescribed slip velocity on the surface R_+ , i.e.,

$$\mathbf{u}|_{|\mathbf{r}|=R_+} = \mathbf{V}(t; \eta) + \mathbf{v}_s, \quad \mathbf{u}|_{|\mathbf{r}|=R_1} = 0. \quad (6)$$

Note that the parametric dependences of the flow field \mathbf{u} on t and η stem from the boundary conditions. Note that because for the outer problem the variations of the flow field and those of the number density of the product molecules are over length scales that are much larger than δ , one can replace everywhere in the calculations the (unknown) value of R_+ by R ; we shall use this approximation in the following.

The solution of the Stokes equations with boundary conditions on spherical surfaces is based on expressing both the flow field \mathbf{u} and the pressure field p as series of solid harmonics^{18,19} $K_l(r, \theta)$ ($l \in \mathbb{Z}$), which are the eigenfunctions of the $3d$ Laplace operator. In Appendix B we provide a brief outline of the general method for solving Eq. (5) in spherical coordinates and derive the solution obeying the BCs given by Eq. 6.

Equation (6) at R_1 corresponds to a no-slip condition imposed on a wall fixed with respect to the laboratory frame. This deserves further discussion. In Eq. (6) the BC is that \mathbf{u} at the surface of the moving particle, i.e., $\mathbf{u}|_{|\mathbf{r}-\mathbf{R}_p(t)|=R_+}$ where $\mathbf{R}_p(t) = \int_0^t \mathbf{V}(t') dt'$ is the position of the particle center, takes the value $\mathbf{V}(t; \eta) + \mathbf{v}_s$. As long as $|\mathbf{R}_p(t)| \ll R_+$, concentricity holds and one obtains the first of the two BCs given by Eq. (6). If, however, the velocity \mathbf{V} is not small, we readjust the center of R_1 in order to impose concentricity using the following ‘‘protocol’’: the particle is allowed to move for a short time δt with the instantaneous velocity $\mathbf{V}(t)$ while the spherical shell at R_1 is fixed, after which the spherical shell is displaced by $\mathbf{V}(t)\delta t$ to its new fixed position in such a way that it does not perturb significantly the density and flow fields; this procedure is then repeated. It is not clear to which extent this latter assumption, which allows us to obtain an analytical solution, can be realized experimentally. But it is expected that the results we derive for the present geometrical setup are relevant also for more general geometries²⁰, such as a particle moving along a channel in $3d$, for which the constraint that the confinement moves with the particle is not needed.

We note that in the general case of a non-spherical particle, or of a particle with non-uniform surface properties (e.g., a spatially varying effective mobility b) the particle can also rotate and the BC at the particle surface, Eq. (6), should include a term accounting for a rigid-body rotation with angular velocity Ω . However, this angular velocity turns out to be identically zero in the case

of a spherical particle with an effective mobility b which is constant on its surface^{12,21}; therefore we completely disregard it here.

3.3. Phoretic velocity

The velocity $\mathbf{V}(t; \eta)$ of the particle is obtained by requiring that the hydrodynamic force

$$\mathbf{F} = \iint_{|\mathbf{r}|=R} \hat{\Pi} \mathbf{e}_r dS, \quad (7)$$

where \mathbf{e}_r is the radial unit vector and dS the surface area element on the spherical surface $|\mathbf{r}| = R$ (note that we replaced R_+ by R , as discussed in the previous subsection), exerted by the fluid on the composite domain particle plus surface film vanishes [see the vector identities in Eq. (B7), (i) - (iii) below this equation, and $(\mathbf{r} \times (\nabla \times \mathbf{u}))_\alpha = x_\beta \partial_\alpha u_\beta - x_\beta \partial_\beta u_\alpha$, with summation over β]:

$$\iint_{|\mathbf{r}|=R} dS \left[-p \mathbf{e}_r + \mu \left(\frac{\partial \mathbf{u}}{\partial r} - \frac{\mathbf{u}}{r} \right) + \frac{\mu}{r} \nabla(\mathbf{r}\mathbf{u}) \right] = 0. \quad (8)$$

If, as discussed above, a rotational motion with angular velocity $\Omega(t; \eta)$ would have to be considered, too, this will be determined by the additional requirement that the motion is not only force free but also torque free¹². This is again due to the fact that there are no net forces acting on the object composed of the particle and its surface film.

The above argument for determining the velocity V has been discussed in detail by Anderson (see Ref. 12 and references therein), but it is often overlooked and replaced by the incorrect argument of a balance between a drag force - i.e., the integral of the non-uniform osmotic pressure proportional to the density of solute (see Appendix A) - exerted on the particle and a Stokes-like viscous friction from the solvent (see, e.g., Refs. 2,22,23). It is important to realize that the occurrence of composition gradients in the solution does not give rise, by itself, to an osmotic pressure (see also Ref. 15), in contrast to such an assumption made in Ref. 22. Such gradients will simply lead to diffusion of the product molecules, while the pressure in the solvent will adjust to accommodate the spatially varying chemical potential corresponding to the quasi-stationary density profile (mildly time dependent due to the overall increase of the solute number density, in the case of the confined system), reflecting mechanical equilibrium¹⁵. As a matter of fact, the origin of this osmotic pressure resides in the interaction between the particle and the product molecules, i.e., it requires the explicit consideration of the effective interaction potential between the particle and the product molecule (for a detailed illuminating discussion of this point see Refs. 12,17). An intuitive argument that the use of such

a ‘‘Stokes-formula’’, which stems from a standard ‘‘drag balanced by viscous friction’’ type of reasoning, is incorrect can be formulated as follows. At distances far from the particle the flow field should look like that produced by the superposition of a point force \mathbf{f} at the origin, i.e., the center of the particle, which is the integrated (over the particle surface) effective ‘‘product molecules on particle’’ interaction (the forces $\hat{\mathbf{f}}_{\mathcal{D}}$ in Fig. 3 in Appendix A), and a distribution of effective point forces oriented radially (of the particle acting on the product molecules) in a small shell region around the surface of the particle (which is the aforementioned surface film), which upon integration gives exactly $-\mathbf{f}$. Note that for repulsive effective interactions and for an axisymmetric distribution of product molecules with an increasing density towards the source at $z = -R$, as in Fig. 1, $\mathbf{f} = \int_S \hat{\mathbf{f}}_{\mathcal{D}} dS$ is oriented into the positive z -direction; for attractive interactions, \mathbf{f} would be oriented into the negative z -direction. This can be seen as follows. For repulsive interactions, each of the forces $\hat{\mathbf{f}}_{\mathcal{D}}$ is oriented radially inwards; since the density of the product molecules is increasing towards the source located on the lower hemisphere, the magnitude and the projection onto the z -direction of the force due to the domain \mathcal{D} located at any $0 < \theta < \pi/2$ is smaller than the one in the corresponding domain \mathcal{D} located at $\pi - \theta$. Thus the contribution into the positive z -direction from the lower hemisphere will dominate. For attractive interactions, the argument is simply reversed. This is in accordance with the following two statements regarding the characteristics of the far-field (i.e., on length scales over which the particle plus surface film are seen as point-like) hydrodynamic flow: (i) In the absence of external body forces such as gravity or centrifugal forces the motion of the particle plus its surface film is net force free. (ii) The generated flow corresponds, within a first approximation, to that produced by a ‘‘force dipole’’ [which is the superposition of a distribution of ‘‘force dipoles’’ ($\hat{\mathbf{f}}_{\mathcal{D}}$ acting on the center and $-\hat{\mathbf{f}}_{\mathcal{D}}$ on the product molecules in \mathcal{D}) as in Fig. 3 in Appendix A], or a higher order ‘‘force multipole’’, e.g., quadrupole (if it happens that the net force dipole vanishes, too)¹⁵ at the origin, i.e., the position of the center of the particle, rather than to the one due to a point force, which would be the case for an object uniformly dragged against the viscous Stokes friction (see, e.g., Ref. 24). For an unbounded system, these forces translate into a radial decay of the phoretic flow field proportional to r^{-2} (force dipole) or r^{-3} (force quadrupole), in contrast to the decay proportional to r^{-1} corresponding to a point force; for a bounded system, the differences between the flow fields cannot be any longer summarized by such a simple criterion as different power laws for the radial decay, but they remain significant nevertheless. These features of the hydrodynamic flow are discussed in more detail in the Appendix B (see also, c.f., Fig. 4).

Using the expansion of the velocity and pressure fields in terms of the solid harmonics K_ℓ (see Appendix B), the

hydrodynamic force on the particle, defined by Eq. (7) and expressed as on the left-hand side of Eq. (8), reduces to

$$\mathbf{F} = 4\pi\tilde{p}_{-2}\nabla[rP_1(\cos\theta)], \quad (9)$$

where \tilde{p}_{-2} is the coefficient of K_{-2} in the expansion of the pressure¹⁸ [Eqs. (B2) and (B3)], and P_1 is the Legendre polynomial of order one. All other terms vanish since the corresponding integrals are exactly equal to zero. Thus the requirement of a vanishing \mathbf{F} implies $\tilde{p}_{-2} = 0$, which leads to (see Appendix B)

$$V(t) = \chi_1(\eta)\frac{b}{R}\int_0^\pi d\theta \sin\theta \cos\theta \rho(R, \theta, t; \eta) \quad (10)$$

where

$$\chi_1(\eta) = 1 - \frac{5\eta^2 - 1}{2\eta^5 - 1}. \quad (11)$$

The structure of the expression on the right-hand side (rhs) of Eq. (10) clarifies the meaning of the factor $\chi_1(\eta)$, which varies between zero, at $\eta \rightarrow 1$, and one, at $\eta \rightarrow \infty$ (see Fig. 2). Without this factor, one has on the rhs the phoretic velocity in the unbounded space due to a source which generates a composition profile ρ_∞ such that $\rho_\infty(R, \theta, t) \equiv \rho(R, \theta, t; \eta)$ at all times t , as derived in Ref. 5 [with $\Lambda \rightarrow -\lambda^2$ entering into b ; see the text around Eq. (4)]. Thus $\chi_1(\eta)$ is a ‘‘hydrodynamic wall-correction’’ factor which quantifies and summarizes the effects solely due to the confinement induced changes in the characteristics of the solvent flow. Note that $\chi_1(\eta) < 1$ means that the hydrodynamic effects due to confinement will tend to decrease the velocity from the value corresponding to an unbounded system.

3.4. Density profile of the product molecules and diffusiophoretic velocity

According to Eq. (10), knowledge of the density $\rho(|\mathbf{r}| = R_+, t; \eta)$ of product molecules completely determines the velocity \mathbf{V} of the particle as a function of $\eta < \infty$ for confined systems and thus allows one to quantify the effects of confinement on the resulting phoretic motion.

Within the assumptions that the diffusion of product molecules is fast compared with the convection by the solvent flow, i.e., in the limit of small Peclet numbers, and that the product distribution $\rho(\mathbf{r}, t)$ is undisturbed by the flow, i.e., neglecting any so-called polarization effects of the surface film¹², the time evolution of the number density $\rho(\mathbf{r}, t)$ of product molecules around the moving particle is governed, in the co-moving frame, by the diffusion equation

$$\partial_t \rho = D\nabla^2 \rho + B(t)\delta(\mathbf{r} - \mathbf{r}_s), \quad R_+ < |\mathbf{r}| < R_1. \quad (12)$$

This equation is to be solved subject to the initial condition (IC) of zero density of product molecules and to the boundary conditions of zero normal current at the confining wall (assuming that the latter is co-moved, without perturbing the solution, such that at all times it remains concentric with the particle) and at the outer edge $r = R_+$ of the surface film. Actually, the latter condition should be imposed at the surface of the particle, but we shall consider only the case of a thin surface film so that due to its small volume the transport of solute to the surface film is negligible compared to the transport in the outer region and the zero normal current condition at R_+ is a good approximation. Hence, the IC and BCs are:

$$\rho(\mathbf{r}, 0) = 0, \quad \left. \left(\frac{\partial \rho(\mathbf{r}, t)}{\partial r} \right) \right|_{|\mathbf{r}|=R_+, R_1} = 0. \quad (13)$$

We remark that the linearity of Eqs. (12) and (10) with respect to ρ imply that by superposition the solution of the present problem can be extended to the case of an arbitrary spatial arrangement of several catalytic sites on the particle surface. This will allow one to find an optimal decoration for providing stability against particle rotations (caused by thermal noise), which can otherwise spoil the unidirectional motion (see Ref. 8 for such examples of designed optimal surface distributions).

Equation (12) subject to the IC and BC conditions given by Eq. (13) is solved by using the Laplace transform. Similarly to the approximation employed in Sec. 3.2, from this point further in the calculations we replace everywhere R_+ by R because the difference δ (the thickness of the surface film) between the two is negligible on the macroscopic length scales characterizing the transport in the outer region. The solution is obtained as a series in products of Legendre polynomials and modified spherical Bessel functions of the first and third kind, respectively; the details are provided in Appendix C. Focusing on the particular case in which after its start the activity of the catalytic site is time independent, i.e., $B(t)$ is constant: $B(t) = H(t)/\tau_f$, where $H(t)$ is the Heaviside step function and τ_f is the average production time for the creation of a product molecule. The Laplace transform of the integral in Eq. (10) is computed by using the Laplace transformed density $\rho(\mathbf{r}, \zeta; \eta)$ and the fact that $\cos\theta = P_1(\cos\theta)$. Formally inverting the Laplace transform, one obtains the diffusiophoretic velocity as a function of time and confinement:

$$V \left(s = \frac{Dt}{R^2}; \eta \right) = \frac{b\chi_1(\eta)}{\pi^2 R^2 D\tau_f} (\mathcal{L}^{-1}[\bar{\Phi}(\xi; \eta)])|_s, \quad (14)$$

where

$$\begin{aligned} \bar{\Phi}(\xi; \eta) &\equiv \frac{i_{3/2}(\sqrt{\xi})}{\sqrt{\xi}} \\ &\times \left[\hat{\alpha}_1 i_{3/2}(\sqrt{\xi}) + (\hat{\beta}_1 - 1) k_{3/2}(\sqrt{\xi}) \right], \quad (15) \end{aligned}$$

$i_{\ell+1/2}(z) = \sqrt{\pi/(2z)}I_{\ell+1/2}(z)$ and $k_{\ell+1/2}(z) = \sqrt{\pi/(2z)}K_{\ell+1/2}(z)$ are modified spherical Bessel functions of the first and third kind, respectively²⁵, and the dimensionless coefficients $\hat{\alpha}_1(\sqrt{\xi}, \eta)$ and $\hat{\beta}_1(\sqrt{\xi}, \eta)$ are fixed by imposing the boundary conditions [see Eq. (C8) and Appendix C with $\xi = \zeta R^2/D$ so that ξ , $\bar{\Phi}$, and $\mathcal{L}^{-1}[\bar{\Phi}]$ are dimensionless].

4. DISCUSSION

The complicated structure of the function $\bar{\Phi}(\zeta; \eta)$ makes it rather laborious to carry out the inverse Laplace transform, so that the full time dependence of the velocity $V(t)$ cannot be derived easily. However, the asymptotic ($s = tD/R^2 \gg 1$) value of the velocity $V^{(\infty)}(\eta) := \lim_{s \rightarrow \infty} V(s; \eta)$ can be straightforwardly derived by using the inversion formula for the Laplace transform²⁶ by noticing that $\bar{\Phi}(\xi; \eta)$ has a simple pole at $\xi = 0$, which determines the asymptotic value of the velocity as the residue of $\bar{\Phi}(\xi; \eta)$ at $\xi = 0$ ²⁶. The existence of such a constant asymptotic value, which at first glance seems to be in conflict with the fact that the density $\rho(\mathbf{r}; t)$ does not reach a steady state (since we consider a closed system with a source continuously producing non-interacting point-like particles), is due to the fact that the phoretic motion is determined solely by the gradient of the number density of the product molecules along the surface of the particle. At long times, the total density of product molecules is large and any redistribution (which would lead to a change of the density gradient) proceeds on very slow time scales. (Ultimately the density of product molecules becomes so high that they no longer behave as an ideal gas and the latter assumption breaks down.) This yields

$$V^{(\infty)}(\eta) = \frac{b\chi_1(\eta)}{\pi^2 R^2 D \tau_f} \text{Res}_{\xi=0} [\bar{\Phi}(\xi; \eta)] = V_0 \chi(\eta), \quad (16)$$

where $V_0 = -\frac{b}{4\pi R^2 D \tau_f} = V^{(\infty)}(\eta \rightarrow \infty)$ is the asymptotic velocity in the case of an unbounded system and [see Eq. (11)]

$$\chi(\eta) = \chi_1(\eta) \frac{\eta^3 + 2}{\eta^3 - 1} := \chi_1(\eta) \chi_2(\eta), \quad \forall \eta > 1. \quad (17)$$

Thus $\chi_2(\eta) = (\eta^3 + 2)/(\eta^3 - 1)$ is a ‘‘diffusion wall-correction’’ factor, and $\chi(\eta)$ quantifies the combined wall effects, which in the present case factorize into a hydrodynamic and a diffusion contribution. These two contributions oppose each other such that the confinement in hydrodynamics decreases the particle velocity ($\chi_1 < 1$) whereas the confinement of the diffusion enhances it ($\chi_2 > 1$) (see Fig. 2); the latter dominates so that $\chi > 1$ and there is an overall enhancement of the velocity (see Fig. 2).

Assuming the Stokes-Einstein relation for the diffusion

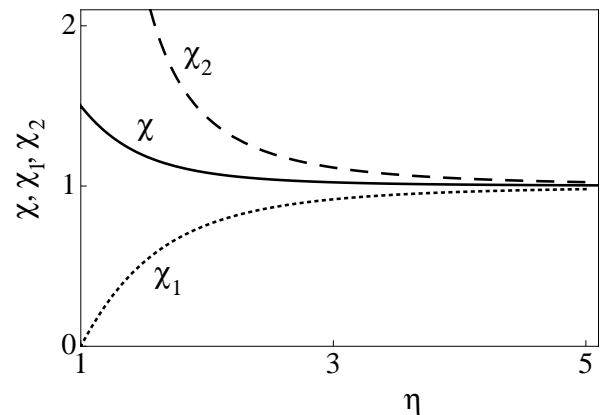


FIG. 2: The long-time asymptotic velocity $V^{(\infty)}(\eta)/V_0 \equiv \chi(\eta) > 1$ (solid line) as a function of the confinement η (see Fig. 1) and the hydrodynamic and diffusion ‘‘wall-correction’’ factors $\chi_1(\eta) < 1$ (dotted line) and $\chi_2(\eta) > 1$ (dashed line).

coefficient of the product molecules in the solvent (see Sec. 1) and using the expression Eq. (3) for the mobility b , the velocity V_0 [Eq. (16)] can be rewritten as

$$V_0 = -\frac{3}{4} \frac{\Lambda}{|\Lambda|} \left(\frac{\lambda}{R} \right)^2 \frac{a}{\tau_f}. \quad (18)$$

Surprisingly, this expression has no explicit dependence on the viscosity of the solvent or on the temperature. In fact, the dependence on viscosity drops out upon using the Stokes-Einstein relation. In turn, the dependence on T is hidden in the temperature dependence of the (effective) interaction between the particle and the product molecules which determines the thickness of the surface film, i.e., the length scale λ [see Eq. (4)]. In the case of only steric repulsion between the particle and the product molecules, for a particle of radius $R = 1 \mu\text{m}$ [100nm], a product molecule with diameter $a = 1.0 \text{ nm}$, $\lambda = 1.0 \text{ nm}$ and a reaction rate (following Ref. 5) of $1/\tau_f = 25 \text{ kHz}$, one finds the velocity $V_0 \simeq 10 \text{ pm/s}$ [1 nm/s]; consequently $V^{(\infty)}(\eta)$ is of the same order of magnitude. Note that these values are much smaller than the estimate $V_0 = \mathcal{O}(\mu\text{m/s})$ of Ref. 5, which is based on a significantly larger value $\lambda^2 \simeq 10^{-15} \text{ m}^2$ than the one $\lambda^2 \simeq 10^{-18} \text{ m}^2$ corresponding to the reasonable estimate $a = 1 \text{ nm}$ for the diameter of the product molecule. However, this estimate corresponds to the case of a single catalytic site. One can argue that several such single reaction sites distributed closely around \mathbf{r}_s may lead to a significant increase of the velocity (intuitively, by a factor equal to the surface density of such reaction sites). Thus the resulting velocities may eventually be closer to the experimentally reported values^{2,6} $V_0 = \mathcal{O}(\mu\text{m/s})$ for objects with a μm^2 area covered by catalyst if the surface density of reaction sites is of the order of nm^{-2} . Moreover, if the effective interaction between the particle and the product molecules is attractive, the ratio $(\lambda/a)^2$ can be very large¹². Another possibility leading to a signif-

icant increase is that of a classical hydrodynamic slip boundary condition with a large slip-length at the surface of the particle for the flow within the surface film, assuming that (see Appendix A) classical hydrodynamics provides an accurate description for the solvent flow even at such small scales¹⁷. (According to the text following Eq. (A5), for the derivation of the effective mobility b in the phoretic slip-velocity [Eqs. (1), (3), and (A6)] we have used a no-slip boundary condition for the flow in the surface film at the particle surface. This condition can be generalized to a slip condition characterized by a slip length.) Such hydrodynamic slip may be, e.g., due to roughness of the particle surface, and its effect on the phoretic motion can be intuitively understood as follows. The slip over the surface of the particle facilitates the solvent flow within the surface film as compared to the case of zero slip (a “lubrication” effect), and thus for the same pressure gradient along the surface as in the case of zero slip the flow velocity in the surface film will be increased for nonzero slip-lengths. The phoretic slip \mathbf{v}_s , which is the flow velocity at the outer boundary of the surface film, is thus also increased compared to its value in the case studied here so far that there is a no-slip condition at the surface of the particle; this leads to an increase (by up to orders of magnitude¹⁷) of the phoretic velocity of the particle.

The velocity $V^{(\infty)}(\eta)$ of the particle can be positive or negative, depending on the details of the interaction potential. This means that the particle can travel either following the gradient of solute density, or against it. According to Eqs. (16) and (18) as well as the definition of the effective mobility b , the sign of the phoretic velocity is opposite to the sign of the parameter b (or, equivalently, that of the parameter Λ), which in turn depends, inter alia, on the attractive or repulsive character of the effective interactions between the particle and the solute molecules [see Eq. (4)]. Equations (1) and (2) show that the sign of the phoretic slip velocity, i.e., of the polar component $\mathbf{v}_s \cdot \mathbf{e}_\theta$ is also opposite to the one of b , because for our system $\partial_\theta \rho$ is positive (see Fig. 1). In the case of hard core interactions only one has $\Lambda < 0$ and thus $b < 0$; this implies $V^{(\infty)}(\eta) > 0$, i.e., the particle moves in the direction of \mathbf{e}_z and thus *away* from the catalytic site, while the slip velocity points in the same direction as \mathbf{e}_θ , which has a negative z -component, so that the flow around the particle is also oriented towards the catalytic site¹². The confinement does not change the direction of \mathbf{V} , which for an unbounded system is, as expected, in agreement with Ref. 5. A simple intuitive explanation for the direction of the motion of the particle follows from the observation that there is no net force acting on the composite consisting of the particle plus the surface film, so that there is conservation of momentum. Because the solvent flow around the particle is in the negative z -direction [see Fig. 4(a)], the particle should move in the positive z -direction. Note that while this simple argument is clear in the unbounded case, for the confined system it breaks down because the formation of

vortices [see Fig. 4(c)] implies that there are spatial regions where the flow is in the positive z -direction. Thus a quantitative analysis is required.

If $b > 0$, on the contrary, $V^{(\infty)}(\eta) < 0$, which means that the particle will move *towards* the source of the product molecules. This is in contrast to the results presented in Ref. 22, which predict motion *always away* from the source. As discussed before the reason for this discrepancy is the ignorance in Ref. 22 of the mediating role of the solvent and its assumption of a mapping of the non-uniform density of the solute onto a non-uniform “osmotic pressure” acting on the particle (i.e., assuming that more product molecules impinge on the particle from the side with higher density), rather than mapping onto gradients in the solution pressure along the surface of the particle within its surface film. This opposing directionality in the case $b > 0$ thus provides a simple criterion for an experimental discrimination between the predictions of the two proposals.

Spatial confinement leads to an overall enhancement of the phoretic motion, because $|V_0| < |V^{(\infty)}(\eta)|$ for all finite η . As shown in Fig. 2, even at moderate values of η the effect of the confinement is important, e.g., at $\eta \simeq 2$ there is a ca. 8% increase in the velocity compared with the unbounded case, and at $\eta \simeq 1.5$ the increase reaches ca. 25%. For $\eta \rightarrow 1$ the velocity stays finite. This is, of course, an artifact which stems from the assumption that the product molecules are point-like. Actually, there is a lower cut-off R_1^c , where $R_1^c - R$ is of the order of the hard core diameter a of the product molecules, below which this assumption breaks down and Eq. (16) is no longer valid. However, for $a \ll R$, which is a reasonable assumption, one has $\eta_c = 1 + a/R \gtrsim 1$, and thus the steep increase of the velocity near $\eta = 1$ is physically relevant. This is a clear counterexample for the statement in the conclusions of Ref. 27 that “the mobility of such swimmers will be hindered by channel boundaries”.

Note that the velocity remains non-zero and finite for all values of η , thus the two opposing effects described by the factors χ_1 and χ_2 are of similar magnitude. This can be understood qualitatively from the behavior of the velocity and density fields in the unbounded system: the hydrodynamic flow velocity decays as r^{-3} , where r is the distance from the center of the particle¹², and the gradients in the number density of product particles (for phoresis the gradients are relevant, not the density in itself) are also varying as⁵ r^{-3} . Accordingly the confinement becomes relevant for both fields at similar length scales and with a similar power-law behavior. Therefore one can expect that the confinement has an equally strong influence on the hydrodynamics and the diffusion.

5. SUMMARY AND CONCLUSIONS

In summary, we have discussed the effect on the phoretic velocity of a self-propelled particle due to a con-

fining wall for the solvent and for the reaction product emerging from a catalytic site on the surface of the dissolved particle.

The analysis is based on considering the present model in the context of the standard theory of phoresis. We have critically analyzed the assumptions involved in such an approach. Some of them are already present in the classical theory, others arise as a result of mapping the description of such “active” surface particles onto the framework of a theory developed to describe the case of inert particles immersed in a pre-defined, externally controlled concentration gradient. For example, within the standard theory of phoresis the perturbation of the steady-state, externally controlled concentration gradient is induced by the interaction with the surface of the particle *upon* immersion. While this is an acceptable concept in that context, it is not clear how one can justify this if the concentration gradient develops as a function of time with the particle already present, as it is the case for a self-propelled object as the one we have discussed. It is beyond the scope of the present work trying to improve the general theory, but we consider a clear understanding of its limitations and of its possible shortcomings as a crucial step for both avoiding confusions such as those involving the application of a Stokes-force argument and for future theoretical developments. The main conclusion from this part of our work is that the development of a microscopic model for the dynamics in the surface film, eventually along the lines of Ref. 7 which treats the solvent and the solute molecules on equal footing, seems to be very important.

Within the confines of the standard theory of phoresis, we have shown that the presence of a confining wall for the solvent and for the reaction product emerging from a catalytic site on the surface of a dissolved particle leads to a significant increase of the velocity of the self-propelled particle. This results from two competing effects: an increase of the solute density gradients along the surface of the particle and a simultaneous increase of the hydrodynamic viscous friction. The former one dominates. If only steric repulsion between the particle and the product molecules is present, the absolute value of the velocity is expected to remain, in general, rather small. A direct experimental realization of the co-moving geometry considered here seems to be difficult. But the results which we have derived are expected to be applicable (at least qualitatively) for more general geometries (see Ref. 20), such as the motion of spherical particles along cylindrical tubes. In this sense, an experimental test of our results may be possible.

Further extensions may focus on new phenomena emerging from more complicated geometries, as well as from relaxing the assumption of no interaction between the product molecules. By taking into account the actual finite size of the product molecules and by considering generic chemical reactions, in which the reaction products are indeed different from the solvent molecules, it is expected that the production of such solute particles

is accompanied by a non-uniform depletion of the solvent around the particle. Thus in general the motion of the particle will be determined by the gradients in both the solvent and the solute (see also Ref. 7). Moreover, such a depletion zone would also lead to a decrease of the production rate of the catalytic site and consequently, to a reduction of the density gradients. Accordingly one might expect that there are optimal values for the reaction rates for which the phoretic velocity is maximal.

The interaction between the product molecules may play a significant role, and this deserves further discussion. If the density of the product particles is not low (which is reasonable to expect at least near the catalytic reaction sites, for fast reactions, and for slow diffusion of product particles) and the (solvent-mediated) solute-solute interactions have attractive or repulsive components longer ranged than the hard-core interaction discussed above, several other effects have to be carefully considered, especially if they are as important as the particle-solute interactions. In this case, the distribution of the solute particles in the direction normal to the surface of the big particle is no longer given by Eq. (A3), but it is determined both by the particle-solute interactions and by the contributions of the solute-solute interactions, the latter depending on the whole distribution of solute particles around the big particle. Thus it becomes a complicated non-local problem which cannot be easily addressed analytically. Within a mean-field approximation, one may still assume that Eq. (A3) holds if the potential is modified to include an averaged, effective solute-solute interaction. It is evident that even such a simplistic approach will lead to a different expression for the phoretic-slip velocity, and thus one can reasonably expect qualitative differences compared to the predictions of the classic theory of phoresis. Moreover, the solute-solute interactions will lead to a dynamics which differs from simple diffusion and is determined, roughly speaking, by the density- and interaction-dependent collective diffusion coefficient. For example, attractive solute-solute interactions will lead to a tendency of “clustering” and thus will hinder the relaxation of the solute gradients, which intuitively would lead to an increase in the velocity of the particle, while repulsive interactions will help to dissipate the particle gradients and, intuitively, would lead to a decrease in the velocity. However, such intuitive arguments for changes in the velocity have to be carefully considered because, e.g., it is not clear if in the presence of significant solute-solute interactions the assumption of an ultrathin “unpolarized” surface film still holds.

Acknowledgments

The authors thank Prof. U. Seifert for very useful remarks concerning the role of the solvent and the phoretic hydrodynamic flow. M.N.P. gratefully acknowledges very fruitful discussions with A. Gambassi, L. Harnau, and M.

Tasinkevych. G.O. acknowledges partial financial support by Agence Nationale de la Recherche (ANR) under the grant “DYOPTRI - Dynamique et Optimisation des Processus de Transport Intermittents”. M.N.P. and G.O. acknowledge the hospitality of the Max-Planck Institute für Metallforschung (MPI-MF) in Stuttgart, as well as partial financial support by the MPI-MF.

APPENDIX A: CALCULATION OF THE PHORETIC SLIP VELOCITY

The following considerations are connected to the corresponding ones in Ref. 12 and put them into the context of the microscopic model discussed in Sect. 2.

Due to the azimuthal symmetry of the system, the flow field $\mathbf{u}(\mathbf{r})$ of the solvent has non-zero components only along the radial and polar directions. According to the considerations in Sect. 2, the dissolved product molecules (solute) of diameter a are exposed to an effective interaction with the particle within a surface film of thickness $\delta \sim a$. Accordingly, the solute molecules do not interact with the particle beyond the radial distance $R_+ = R + \delta$ (measured from the center O of the particle). Since the particle radius R is much larger than a so that $\delta/R \ll 1$, this surface film of thickness δ can be approximated to be locally planar (see Fig. 3). In a small domain \mathcal{D} centered at $\mathbf{r} = (R, \theta, \phi)$ (Fig. 3), the local coordinate system $(\hat{\cdot})$ is chosen such that \hat{x} is along the polar direction \mathbf{e}_θ while \hat{y} is along the radial (normal) direction \mathbf{e}_r .

Within the planar film approximation, which is reliable because the film thickness δ is taken to be much smaller than the particle radius R ($\delta \ll R$), and for slow and smooth variations of the solute density along the surface of the particle (i.e., the solute density is assumed to vary over length scales of the order of the particle radius R), the flow of the solvent relative to the particle surface is $\hat{\mathbf{u}}(\hat{x}, \hat{y}) \simeq (\hat{u}_{\hat{x}}(\hat{x}, \hat{y}), 0)$ (with the meaning that the ratio $\hat{u}_{\hat{y}}/\hat{u}_{\hat{x}}$ is of the order $\mathcal{O}(\delta/R) \ll 1$)¹². This can be intuitively understood starting from the incompressibility condition $\hat{\nabla} \cdot \hat{\mathbf{u}} = 0$, where $\hat{\nabla}$ indicates that the derivatives are taken with respect to the local coordinates. The component $\hat{u}_{\hat{x}}$ is of the order of the slip velocity $|\mathbf{v}_s|$, which is expected to be proportional to the gradient along the surface, i.e., along the \hat{x} direction, of the solute density ρ evaluated at R_+ . Noting that $d\hat{x} = R d\theta$, one obtains $\partial_{\hat{x}} \hat{u}_{\hat{x}} \sim (1/R^2) \partial_\theta^2 \rho$. On the other hand, the component $\hat{u}_{\hat{y}}$ has to rise steeply within the surface film of thickness δ from the value zero at the surface of the particle to the value corresponding to the radial component of the outer flow, which is expected to be also of the order of $|\mathbf{v}_s|$. Therefore $\partial_{\hat{y}} \hat{u}_{\hat{y}} \sim |\mathbf{v}_s|/\delta \sim [1/(R\delta)] \partial_\theta \rho$. Since the derivatives of the solute density profiles with respect to θ are expected to not depend on the surface film thickness δ and to be finite (due to assumed smooth, slow variations over length scales of the order of the particle radius), it follows that $\partial_{\hat{y}} \hat{u}_{\hat{y}}/\partial_{\hat{x}} \hat{u}_{\hat{x}} \sim R/\delta$ so that $|\partial_{\hat{y}} \hat{u}_{\hat{y}}| \gg |\partial_{\hat{x}} \hat{u}_{\hat{x}}|$. Thus the incompressibility condition $\partial_{\hat{x}} \hat{u}_{\hat{x}} + \partial_{\hat{y}} \hat{u}_{\hat{y}} = 0$ im-

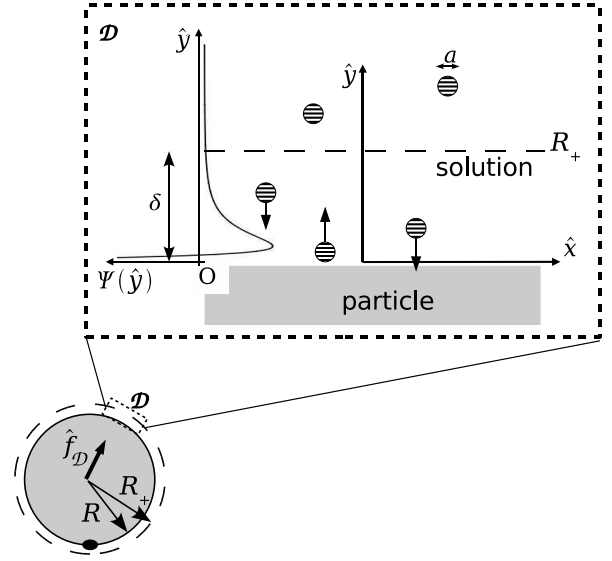


FIG. 3: Schematic expanded view of a domain \mathcal{D} of the contact region between the particle and the solution, far from the reaction site, approximated locally by a planar geometry. The effective interaction between the reaction products, shown as horizontally hatched circles, and the particle is described by an effective potential $\Psi(\hat{y})$; \hat{y} is the normal distance from the surface of the particle, also schematically depicted. The arrows at the product molecules indicate the forces $-\nabla\Psi(\hat{y})$ acting on them, while the arrow at the particle center shows the force $\hat{f}_{\mathcal{D}}$ on it, due to the same interaction with the product molecules, which is equal in magnitude and opposite to the sum of $-\nabla\Psi(\hat{y})$ over the product molecules positions in \mathcal{D} . Here the case is shown that the product molecules in \mathcal{D} exert a net attractive force on the particle. The “outer edge” R_+ of the surface film beyond which the effective interactions between the particle and the product molecules are negligible is indicated by the horizontal dashed line. The solvent, within which the product molecules move, is taken to be a homogeneous background (not shown). Actually, $\delta = R_+ - R$ (of the order of the product molecules diameter a) is considered to be smaller than indicated here.

plies that the leading contribution $\sim 1/(R\delta)$ must vanish separately because it cannot be canceled by subleading contributions $\sim 1/R^2$. Therefore one has $\partial_{\hat{y}} \hat{u}_{\hat{y}} \simeq 0$ (up to terms of relative order $\mathcal{O}(\delta/R)$). This implies that $\hat{u}_{\hat{y}}$ does not depend on \hat{y} ; because $\hat{u}_{\hat{y}} = 0$ on the surface of the particle (independently of \hat{x}), due to the surface being impermeable, it follows that $\hat{u}_{\hat{y}} \simeq 0$ (in the sense of correction terms $\sim \delta/R$) everywhere in \mathcal{D} .

As indicated in Fig. 3, the effective interaction of the product molecules (solute) with the particle, characterized by the effective interaction potential $\Psi(\hat{y})$ (in the limit of low solute density many-body effects can be ignored so that Ψ is independent of \hat{x}), gives rise to a force $-\nabla\Psi$ acting on the solute molecules. Assuming that the solvent can be approximated as a continuum on the length scale of the solute, the no-slip condition at the surface of the *solute* molecules implies that a body force density $-\rho\nabla\Psi$ is transmitted to the solvent. (Note

that, as discussed also in the main text, the approximation of the solvent as a continuum breaks down if the solute molecules have a size similar to that of the solvent molecules, as in the case of the experiments discussed in Refs. 1,6; in such a case this transmission of the body force has to be considered as an assumption to be verified *a posteriori*.) Evidently, such forces are present only within the surface film, where the effective interaction potential is non-zero. Within these assumptions, the Stokes equations for the flow $\hat{\mathbf{u}}(\hat{x}, \hat{y}) \simeq (\hat{u}_x(\hat{x}, \hat{y}), 0)$ within the surface film take on the form:

$$\mu \hat{\nabla}^2 \hat{\mathbf{u}} = \hat{\nabla} p + \rho \hat{\nabla} \Psi. \quad (\text{A1})$$

The equation corresponding to the \hat{x} component of Eq. (A1) can be further simplified by noting (with an argument similar to the one used in the paragraph above) that the partial derivative $|\partial_{\hat{x}}^2 \hat{u}_x|$ is much smaller than $|\partial_{\hat{y}}^2 \hat{u}_x|$ (by a factor of the order $\mathcal{O}[(\delta/R)^2]$). Thus for the \hat{x} component Eq. (A1) leads to

$$\mu \partial_{\hat{y}}^2 \hat{u}_x = \partial_{\hat{x}} p, \quad (\text{A2a})$$

whereas the \hat{y} component yields

$$\partial_{\hat{y}} p = -\rho(\hat{x}, \hat{y}) \partial_{\hat{y}} \Psi. \quad (\text{A2b})$$

We further assume that within the very thin surface film the relaxation of the solute density profile along the direction normal to the surface of the self-propelled particle towards a steady-state (zero net current, i.e., the diffusion current due to gradients in ρ along the \hat{y} direction is balanced by the convective current generated by the force-field $-\nabla \Psi$) is fast compared to the diffusional relaxation time of its gradient along the surface^{12,17}. In this case, *within* the surface film the number density of the solute, assumed to behave like an ideal gas, is given by the Boltzmann distribution corresponding to the effective interaction $\Psi(\hat{y})$:

$$\rho(\hat{x}, \hat{y}) \simeq \rho(\hat{x}, R_+) e^{-\beta \Psi(\hat{y})}. \quad (\text{A3})$$

(The prefactor $\rho(\hat{x}, R_+)$ reflects the fact that $\Psi(\hat{y} \rightarrow \delta)$ becomes negligibly small; we emphasize that Eq. (A3) applies *only within* the surface film.) We note that this assumption can break down, especially in the immediate vicinity of the reaction site, if the reaction rate is high. In such a case one has to explicitly consider the coupled equations of mass transport for the solvent and solute within the surface film (see Ref. 7); as already mentioned before, we consider here only situations in which Eq. (A3) holds.

Combining Eqs. (A2b) and (A3), integrating with respect to \hat{y} , and using that the inner and outer solutions for the hydrodynamic flow should match smoothly at R_+ so that at R_+ the pressure reaches its “outer” solution value $p_{\text{out}}(\hat{x}, \hat{y} = R_+)$, one obtains the following expres-

sion for the pressure field within the surface film:

$$p(\hat{x}, \hat{y}) = p_{\text{out}}(\hat{x}, R_+) + k_B T [\rho(\hat{x}, \hat{y}) - \rho(\hat{x}, R_+)]. \quad (\text{A4})$$

This is the so-called “osmotic equilibrium” condition (because on the right hand side the term after the plus sign has the form known as “osmotic pressure”) along the surface normal, which varies along the surface of the particle due to the gradient in the solute density^{12,17}. Note that Eq. (A4) also applies *only within* the surface film.

By: (i) combining Eqs. (A2a), (A3), and (A4), (ii) noting that $\partial_{\hat{x}} p_{\text{out}}(\hat{x}, R_+)$ can be neglected because $\partial_{\hat{x}} p_{\text{out}}(\hat{x}, R_+) \sim \mu |\mathbf{v}_s| / R^2$ (this is because the outer solution satisfies the force-free ($\Psi = 0$) version of Eq. (A1); by evaluating it at R_+ and along the surface of the particle and by noting that the slip velocity varies over the macroscopic length scale R , the above conclusion follows) while with $|\hat{u}_x(\hat{y} = R_+)| = |\mathbf{v}_s|$ and $\hat{u}_x(\hat{y} = 0) = 0$ one finds from Eq. (A2a) that $\partial_{\hat{x}} p(\hat{x}, R_+) \sim \mu |\mathbf{v}_s| / \delta^2$, (iii) introducing

$$h(\hat{x}, \hat{y}) := \frac{k_B T}{\mu} \frac{d\rho(\hat{x}, R_+)}{d\hat{x}} \left(e^{-\beta \Psi(\hat{y})} - 1 \right),$$

(iv) integrating once, and (v) using $\partial_{\hat{y}} \hat{u}_x|_{R_+} = 0$ (which holds because the inhomogeneity causing the flow vanishes at the outer edge of the surface film), one obtains

$$\partial_{\hat{y}} \hat{u}_x = - \int_{\hat{y}}^{R_+} du h(\hat{x}, u) =: -g(\hat{x}, \hat{y}). \quad (\text{A5})$$

Integrating by parts, using the boundary condition $\hat{u}_x(\hat{y} = 0) = 0$ of no-slip at the particle surface, and noting that $u g(\hat{x}, u) \rightarrow 0$ for $u \rightarrow 0$ (because $h(\hat{x}, u)$ is bounded with respect to u , so that $g(\hat{x}, u)$ is finite for all u) and $g(\hat{x}, R_+) = 0$ [by definition of $g(\hat{x}, \hat{y})$], one obtains the phoretic slip-velocity $\mathbf{v}_s = \hat{u}_x(\hat{x} = R_+\theta, R_+) \mathbf{e}_\theta$ as

$$\mathbf{v}_s(\theta) = -\mathbf{e}_\theta \int_0^{R_+} du u h(\hat{x} = R_+\theta, u). \quad (\text{A6})$$

Since $h(\hat{x}, u)$ decays rapidly for $u > R_+$ the integral in Eq. (A6) can be extended to infinity without causing a significant error:

$$\begin{aligned} \mathbf{v}_s(\theta) &\simeq -\mathbf{e}_\theta \frac{k_B T}{\mu} \frac{d\rho(\hat{x}, R_+)}{d\hat{x}} \int_0^\infty du u [e^{-\beta \Psi(u)} - 1] \\ &= -\mathbf{e}_\theta b \frac{d\rho(\hat{x} = R_+\theta, R_+)}{d\hat{x}}. \end{aligned} \quad (\text{A7})$$

The derivation of the expression for the phoretic slip-velocity is concluded by noting that $\frac{d\rho}{d\hat{x}} = \frac{1}{R_+} \frac{d\rho}{d\theta}$ corresponds to the gradient of the solute number density along the particle surface [see Eqs. (1)-(4)].

**APPENDIX B: CALCULATION OF THE
HYDRODYNAMIC FLOW IN THE OUTER
REGION (BEYOND THE SURFACE FILM)
AND OF THE HYDRODYNAMIC FORCE**

A general solution for the three-dimensional steady-state force-free Stokes equations,

$$\mu \nabla^2 \mathbf{u} = \nabla p, \quad (\text{B1a})$$

$$\nabla \mathbf{u} = 0, \quad (\text{B1b})$$

in spherical coordinates has been obtained by Lamb^{18,19}. Here we briefly present the derivation, adapted to the present case which has an additional azimuthal symmetry, and we also compute the hydrodynamic force in the case of a flow subject to the boundary conditions given by Eq. (6).

The general solution is written as $\mathbf{u} = \mathbf{u}_{hom} + \mathbf{u}_p$, where \mathbf{u}_{hom} is the solution of the homogeneous equations, i.e., $\mu \nabla^2 \mathbf{u}_{hom} = 0$ (so that the components of \mathbf{u}_{hom} are harmonic functions, i.e., they obey the Laplace equation) and $\nabla \mathbf{u}_{hom} = 0$, while \mathbf{u}_p is a particular solution of Eqs. (B1a) and (B1b).

1. General solution in spherical coordinates in the presence of azimuthal symmetry

The calculation of \mathbf{u} proceeds by separately determining the components \mathbf{u}_{hom} and \mathbf{u}_p defined above. The construction of the component $\mathbf{u}_p(r, \theta)$ [a particular solution of the inhomogeneous Eq. (B1a)] starts from the observation that the pressure field is also a harmonic function, i.e., $\nabla^2 p = 0$ [this follows from taking the divergence of Eq. (B1a)]. Therefore, it can be expanded in terms of the solid harmonics¹⁸, which are the eigenfunctions of the Laplace operator in $3d$:

$$p(r, \theta) = \sum_{\ell \in \mathbb{Z}} \tilde{p}_\ell K_\ell(r, \theta), \quad (\text{B2})$$

where

$$K_\ell(r, \theta) = r^\ell Q_\ell(\cos \theta), \ell \in \mathbb{Z}, \quad (\text{B3})$$

with

$$Q_\ell(\cos \theta) = \begin{cases} P_\ell(\cos \theta), & \text{for } \ell \geq 0, \\ P_{|\ell-1}(\cos \theta), & \text{for } \ell < 0, \end{cases} \quad (\text{B4})$$

and $P_\ell(\cos \theta)$ is the Legendre polynomial of degree ℓ .

In this representation, a particular solution \mathbf{u}_p is given by^{18,19}

$$\mathbf{u}_p = \sum_{\ell \in \mathbb{Z}} \tilde{p}_\ell [A_\ell r^2 \nabla K_\ell + B_\ell \mathbf{r} K_\ell] \quad (\text{B5})$$

where

$$A_\ell = \frac{\ell + 3}{2\mu(\ell + 1)(2\ell + 3)}, \quad B_\ell = -\frac{2\ell}{\ell + 3} A_\ell. \quad (\text{B6})$$

This can be checked by inserting Eqs. (B5) and (B6) into Eqs. (B1a, b) and by noting that $\nabla \mathbf{r} = 3$ and $r \partial_r K_\ell = \ell K_\ell$. Note that the pole in A_ℓ at $\ell = -1$ is cancelled in Eq. (B5).

The construction of the solution \mathbf{u}_{hom} starts from the identity

$$\begin{aligned} \nabla(\mathbf{r} \mathbf{u}_{hom}) &= \mathbf{r} \times (\nabla \times \mathbf{u}_{hom}) + \mathbf{u}_{hom} \times (\nabla \times \mathbf{r}) \\ &+ (\mathbf{u}_{hom} \cdot \nabla) \mathbf{r} + (\mathbf{r} \cdot \nabla) \mathbf{u}_{hom}. \end{aligned} \quad (\text{B7})$$

Expressing the vorticity $\nabla \times \mathbf{u}_{hom}$ as $\nabla \Upsilon$ [this is possible because $\nabla \times (\nabla \times \mathbf{u}_{hom}) = \nabla(\nabla \cdot \mathbf{u}_{hom}) - \nabla^2 \mathbf{u}_{hom} = 0$] and denoting the product $\mathbf{r} \cdot \mathbf{u}_{hom}$ by Φ , and noting that: (i) $\nabla \times \mathbf{r} = 0$; (ii) $(\mathbf{u}_{hom} \cdot \nabla) \mathbf{r} = \mathbf{u}_{hom}$; (iii) $(\mathbf{r} \cdot \nabla) \mathbf{u}_{hom} = r \partial_r \mathbf{u}_{hom}$; (iv) $\mathbf{r} \times (\nabla \Upsilon) = -\nabla \times (\mathbf{r} \Upsilon)$, Eq. (B7) can be re-written as

$$\mathbf{u}_{hom} + r \partial_r \mathbf{u}_{hom} = \nabla \Phi + \nabla \times (\mathbf{r} \Upsilon). \quad (\text{B8})$$

Due to $\nabla \times \mathbf{u}_{hom} = \nabla \Upsilon$ one has $\nabla^2 \Upsilon = 0$ so that Υ is harmonic, and due to $\nabla^2 \Phi = 2 \nabla \cdot \mathbf{u}_{hom} + \mathbf{r} \cdot (\nabla^2 \mathbf{u}_{hom}) = 0$ also Φ is a harmonic function. By inserting the series expansions in solid harmonics [compare Eq. (B2)] of \mathbf{u}_{hom} , Υ , and Φ into Eq. (B8) and by using $r \partial_r K_\ell = \ell K_\ell$, one finds that the solution \mathbf{u}_{hom} is given by

$$\mathbf{u}_{hom} = \sum_{\ell \in \mathbb{Z}} [\tilde{\Upsilon}_\ell \nabla \times (\mathbf{r} K_\ell) + \tilde{\Phi}_\ell \nabla K_\ell], \quad (\text{B9})$$

where $\tilde{\Upsilon}_\ell$ and $\tilde{\Phi}_\ell$ are the corresponding expansion coefficients of Υ and Φ as in Eq. (B2).

The sum of Eqs. (B5) and (B9) provides the general solution $\mathbf{u} = \mathbf{u}_p + \mathbf{u}_{hom}$ expressed as a series expansion in spherical harmonics^{18,19} with the coefficients $\{\tilde{p}_\ell, \tilde{\Upsilon}_\ell, \tilde{\Phi}_\ell\}$ determined by boundary conditions *on spherical surfaces*. Note that for a problem without azimuthal symmetry the derivation of the solution proceeds analogously and the only change is that the Legendre polynomials $P_\ell(\cos \theta)$ ($\ell \geq 0$) are replaced everywhere by a linear combination (with respect to the index $-\ell \leq m \leq \ell$) of the spherical harmonics $Y_{\ell m}(\theta, \phi)$.

2. Boundary conditions for problems with spherical symmetry

The general solution derived in the previous subsection allows one to determine the hydrodynamic flow obeying Eqs. (B1a, b) in a spherical domain with prescribed velocity on the boundaries of the domain (or at infinity). This is carried out in the usual manner by expanding the prescribed surface fields in terms of Legendre polynomials and then equating them with the series representation of the general solution evaluated at the boundary to de-

termine the expansion coefficients $\{\tilde{p}_\ell, \tilde{\Upsilon}_\ell, \tilde{\Phi}_\ell\}$. However, the prescribed boundary conditions for velocity fields can be used to obtain an equivalent set of boundary conditions, which exploits the simplicity of the derivatives of the solid harmonics with respect to the radial coordinate and thus significantly simplifies the algebra¹⁸; here we follow this approach, and discuss the most general case, i.e., without azimuthal symmetry.

Let \mathbf{U} denote the prescribed velocity field on a spherical boundary $|\mathbf{r}| = c$, i.e., $\mathbf{u}(r = c, \theta, \phi) = \mathbf{U}(\theta, \phi)$; in our case $\mathbf{U} = \mathbf{V} + \mathbf{v}_s$ for $c = R_+$ and $\mathbf{U} = 0$ for $c = R_1$.

(i) By multiplying $\mathbf{u}(r = c, \theta, \phi) = \mathbf{U}(\theta, \phi)$ with \mathbf{e}_r , one obtains the radial component u_r of the flow field

$$u_r(r = c, \theta, \phi) = \mathbf{e}_r \cdot \mathbf{U}(\theta, \phi) =: U_r(\theta, \phi), \quad (\text{B10})$$

where U_r denotes the radial component of the velocity \mathbf{U} prescribed at the spherical boundary.

(ii) The radial component of the vorticity is given by

$$\mathbf{e}_r \cdot (\nabla \times \mathbf{u}) = \frac{1}{r \sin \theta} [\partial_\theta (\sin \theta u_\phi) - \partial_\phi u_\theta], \quad (\text{B11})$$

where u_θ and u_ϕ are the polar and azimuthal components of \mathbf{u} , respectively. On the spherical boundary $|\mathbf{r}| = c$, within the right hand side of Eq. (B11) u_ϕ and u_θ can be replaced by U_ϕ and U_θ , respectively. Thus the radial component of the vorticity obeys

$$\begin{aligned} [\mathbf{r} \cdot (\nabla \times \mathbf{u})]_{r=c} &= \mathbf{r} \cdot (\nabla \times \mathbf{U}) \\ &= \frac{1}{\sin \theta} [\partial_\theta (\sin \theta U_\phi) - \partial_\phi U_\theta]. \end{aligned} \quad (\text{B12})$$

(iii) Since $\nabla \mathbf{u} = 0$, one has

$$\begin{aligned} 0 = r \nabla \mathbf{u} &= r \partial_r u_r + 2u_r \\ &+ \frac{1}{\sin \theta} [\partial_\theta (\sin \theta u_\theta) + \partial_\phi u_\phi]. \end{aligned} \quad (\text{B13})$$

Since $\partial_r U_r(\theta, \phi) = 0$, $u_\theta(r = c, \theta, \phi) = U_\theta(\theta, \phi)$, and $u_\phi(r = c, \theta, \phi) = U_\phi(\theta, \phi)$, Eq. (B13) renders on $|\mathbf{r}| = c$ the boundary condition

$$[r \partial_r u_r]_{r=c} = -r(\nabla \mathbf{U}). \quad (\text{B14})$$

Determining u_r , $\mathbf{r} \cdot (\nabla \times \mathbf{u})$, and $r \partial_r u_r$ from the solution $\mathbf{u} = \mathbf{u}_{hom} + \mathbf{u}_p$ [Eqs. (B5) and (B9)], evaluating the expressions at $r = c$, and equating them to the rhs of Eqs. (B10), (B12), and (B14), respectively, after expanding the latter in terms of spherical harmonics, yields the equations of condition for the coefficients $\{\tilde{p}_\ell, \tilde{\Upsilon}_\ell, \tilde{\Phi}_\ell\}$. Applying this procedure for all boundaries, combining all the resultant conditions, and solving for the coefficients $\{\tilde{p}_\ell, \tilde{\Upsilon}_\ell, \tilde{\Phi}_\ell\}$ yields the velocity \mathbf{u} in terms of $\mathbf{U}(\theta, \phi) = \mathbf{u}(r = c, \theta, \phi)$.

3. The outer hydrodynamic flow

We now apply the general results discussed in the previous subsections to the particular confined system shown in Fig. 1, which exhibits azimuthal symmetry and obeys the boundary conditions in Eq. (6) on the spherical surfaces $|\mathbf{r}| = R_+ \simeq R$ and $R_1 = \eta R$, respectively. Using the expansion of $\mathbf{u} = \mathbf{u}_p + \mathbf{u}_{hom}$ in terms of solid harmonics [Eqs. (B5) and (B9)] and exploiting the azimuthal symmetry (i.e., the solution does not depend on ϕ), splitting this series into two, corresponding to $\ell \geq 0$ and $\ell < 0$, respectively, changing in the latter the index of summation according to $\ell \mapsto -(n+1)$, $n \geq 0$, and then renaming n by ℓ , one obtains¹⁸

$$\begin{aligned} u_r &= \sum_{\ell \geq 0} \left[\frac{\ell}{2\mu(2\ell+3)} r^{\ell+1} \tilde{p}_\ell + \frac{\ell+1}{2\mu(2\ell-1)r^\ell} \tilde{p}_{-(\ell+1)} \right. \\ &\quad \left. + \ell r^{\ell-1} \tilde{\Phi}_\ell - \frac{\ell+1}{r^{\ell+2}} \tilde{\Phi}_{-(\ell+1)} \right] P_\ell(\cos \theta), \end{aligned} \quad (\text{B15a})$$

$$r(\nabla \times \mathbf{u})_r = \sum_{\ell \geq 0} \ell(\ell+1) \left[r^\ell \tilde{\Upsilon}_\ell + \frac{\tilde{\Upsilon}_{-(\ell+1)}}{r^{\ell+1}} \right] P_\ell(\cos \theta), \quad (\text{B15b})$$

$$\begin{aligned} r \partial_r u_r &= \sum_{\ell \geq 0} \left[\frac{\ell(\ell+1)}{2\mu(2\ell+3)} r^{\ell+1} \tilde{p}_\ell - \frac{\ell(\ell+1)}{2\mu(2\ell-1)r^\ell} \tilde{p}_{-(\ell+1)} \right. \\ &\quad \left. + \ell(\ell-1)r^{\ell-1} \tilde{\Phi}_\ell + \frac{(\ell+1)(\ell+2)}{r^{\ell+2}} \tilde{\Phi}_{-(\ell+1)} \right] P_\ell(\cos \theta). \end{aligned} \quad (\text{B15c})$$

Equations (B15a), (B15b), and (B15c) relate to Eqs. (B10), (B12), and (B14), respectively. The rhs of Eqs. (B15a) and (B15c) do not depend on the coefficients $\{\tilde{\Upsilon}_\ell\}$ because the contributions $\tilde{\Upsilon}_\ell \nabla \times (\mathbf{r} K_\ell)$ in Eq. (B9) have no radial component. Similarly, the rhs of Eq. (B15b) does not depend on $\{\tilde{p}_\ell\}$ and $\{\tilde{\Phi}_\ell\}$ because $\mathbf{r} \cdot (\nabla \times \mathbf{u}_p) = 0$ [Eq. (B5)] and $\nabla \times (\nabla K_\ell) = 0$ [Eq. (B9)], respectively.

By noting that $\nabla \mathbf{V} = 0$, $\nabla \times \mathbf{V} = 0$ [because the particle velocity $\mathbf{V} = V \mathbf{e}_z$ depends only on t and η , see Eq. (10)], and $\nabla \times \mathbf{v}_s = 0$ [because the slip velocity is given by a gradient, see Eq. (1)], one obtains that on the spherical surface $|\mathbf{r}| = R_+ \simeq R$ one has [see Eq. (B10)] $U_r = (\mathbf{V} + \mathbf{v}_s)_r = V \cos \theta$ [because $\mathbf{V} = V \mathbf{e}_z$ and $\mathbf{e}_r \cdot \mathbf{v}_s = 0$, see Eq. (A6)], $\mathbf{r} \cdot [\nabla \times \mathbf{U}] = \mathbf{r} \cdot [\nabla \times (\mathbf{V} + \mathbf{v}_s)] = 0$ [see Eq. (B12)], and [see Eq. (B14)]

$$-r \nabla \mathbf{U} = -r \nabla (\mathbf{V} + \mathbf{v}_s) = -r \nabla \mathbf{v}_s = -k(\theta, R), \quad (\text{B16})$$

where [due to $\mathbf{v}_s = -b \nabla_s \rho(R, \theta; t, \eta)$]

$$\begin{aligned} k(\theta, R) &= -\frac{b}{R \sin \theta} \partial_\theta (\sin \theta \partial_\theta \rho) \\ &= \sum_{\ell \geq 0} \tilde{k}_\ell(R) P_\ell(\cos \theta), \end{aligned} \quad (\text{B17})$$

ρ denotes $\rho(R, \theta; t, \eta)$, and

$$\begin{aligned} \tilde{k}_\ell(R) &= \frac{2\ell+1}{2} \int_0^\pi d\theta \sin\theta k(\theta, R) P_\ell(\cos\theta) \\ &= \frac{2\ell+1}{2} \frac{b}{R} \int_0^\pi d\theta \sin\theta \frac{\partial\rho}{\partial\theta} \frac{dP_\ell(\cos\theta)}{d\theta}. \end{aligned} \quad (\text{B18})$$

(The last equality follows upon integrating by parts.) By evaluating the right hand sides of Eqs. (B15a), (B15b), and (B15c) at R and R_1 and equating them on the left hand sides with $V \cos(\theta)$, 0 , $-k(\theta, R)$ and with 0 , 0 , 0 , respectively, the coefficients $\{\tilde{p}_\ell, \tilde{\Upsilon}_\ell, \tilde{\Phi}_\ell\}$ are obtained for any $\ell \geq 0$ as the solution of the system of equations given by

$$\begin{aligned} \frac{\ell R^{\ell+1}}{2\mu(2\ell+3)} \tilde{p}_\ell + \frac{\ell+1}{2\mu(2\ell-1)R^\ell} \tilde{p}_{-(\ell+1)} \\ + \ell R^{\ell-1} \tilde{\Phi}_\ell - \frac{\ell+1}{R^{\ell+2}} \tilde{\Phi}_{-(\ell+1)} = V \delta_{\ell,1}, \end{aligned} \quad (\text{B19a})$$

$$R^\ell \tilde{\Upsilon}_\ell + \frac{\tilde{\Upsilon}_{-(\ell+1)}}{R^{\ell+1}} = 0, \quad (\text{B19b})$$

$$\begin{aligned} \frac{\ell(\ell+1)R^{\ell+1}}{2\mu(2\ell+3)} \tilde{p}_\ell - \frac{\ell(\ell+1)}{2\mu(2\ell-1)R^\ell} \tilde{p}_{-(\ell+1)} \\ + \ell(\ell-1)R^{\ell-1} \tilde{\Phi}_\ell + \frac{(\ell+1)(\ell+2)}{R^{\ell+2}} \tilde{\Phi}_{-(\ell+1)} = -\tilde{k}_\ell(R), \end{aligned} \quad (\text{B19c})$$

$$\begin{aligned} \frac{\ell R_1^{\ell+1}}{2\mu(2\ell+3)} \tilde{p}_\ell + \frac{\ell+1}{2\mu(2\ell-1)R_1^\ell} \tilde{p}_{-(\ell+1)} \\ + \ell R_1^{\ell-1} \tilde{\Phi}_\ell - \frac{\ell+1}{R_1^{\ell+2}} \tilde{\Phi}_{-(\ell+1)} = 0, \end{aligned} \quad (\text{B19d})$$

$$R_1^\ell \tilde{\Upsilon}_\ell + \frac{\tilde{\Upsilon}_{-(\ell+1)}}{R_1^{\ell+1}} = 0, \quad (\text{B19e})$$

$$\begin{aligned} \frac{\ell(\ell+1)R_1^{\ell+1}}{2\mu(2\ell+3)} \tilde{p}_\ell - \frac{\ell(\ell+1)}{2\mu(2\ell-1)R_1^\ell} \tilde{p}_{-(\ell+1)} \\ + \ell(\ell-1)R_1^{\ell-1} \tilde{\Phi}_\ell + \frac{(\ell+1)(\ell+2)}{R_1^{\ell+2}} \tilde{\Phi}_{-(\ell+1)} = 0. \end{aligned} \quad (\text{B19f})$$

Note that Eqs. (B19b) and (B19e) imply that $\tilde{\Upsilon}_\ell = \tilde{\Upsilon}_{-\ell} = 0$ for all ℓ . Therefore, for any given ℓ one is left with a linear system of four equations for four unknowns: $\tilde{p}_\ell, \tilde{\Phi}_\ell, \tilde{p}_{-(\ell+1)}, \tilde{\Phi}_{-(\ell+1)}$, which (in the generic case) admits a unique solution.

Taking $\ell = 1$ in Eq. (B19), one obtains a system of

four linear equations for the unknowns $\tilde{p}_1, \tilde{\Phi}_1, \tilde{p}_{-2}, \tilde{\Phi}_{-2}$, which depend parametrically on V, R, R_1 , and μ [see Eq. (B6)]. The absence of a body force acting on the particle implies \tilde{p}_{-2} [see Eqs. (7) - (9)]. This leads to:

$$V = \frac{\tilde{k}_1(R)}{3} \left[1 - \frac{5\eta^2 - 1}{2\eta^5 - 1} \right]. \quad (\text{B20})$$

By noting that

$$\begin{aligned} \tilde{k}_1(R) &= \frac{3b}{2R} \int_0^\pi d\theta \sin\theta \frac{\partial\rho}{\partial\theta} \frac{dP_1(\cos\theta)}{d\theta} \\ &= -\frac{3b}{2R} \int_0^\pi d\theta \sin^2\theta \frac{\partial\rho}{\partial\theta} \\ &= 3\frac{b}{R} \int_0^\pi d\theta \sin\theta \cos\theta \rho(R, \theta), \end{aligned} \quad (\text{B21})$$

one obtains the expression Eq. (10) in the main text. Because $\partial_\theta \rho$ is positive for the system depicted in Fig. 1 the second equality in Eq. (B21) implies that the sign of $\tilde{k}_1(R)$, and therefore that of V [see Eq. (B20)], is opposite to the one of the effective mobility b .

Before concluding this appendix, we note that the general solution for the hydrodynamic flow [Eqs. (B5), (B9), and (B19)] allows one to gain insight into the qualitative differences between the phoretic motion mechanism and the one of an ‘‘osmotic pressure’’ propeller²². In Figs. 4(a) and (c) we show the normalized velocity fields $\mathbf{u}/|\mathbf{u}|$ corresponding to diffusiophoretic motion due to steric repulsion only. In this case $b < 0$ [see Eq. (4)] so that the particle velocity $\mathbf{V} = V\mathbf{e}_z$ is oriented along the positive z -direction, i.e., away from the source. Figure 4(a) corresponds to an unbounded system whereas Fig. 4(c) depicts the corresponding confined system with $\eta = 5$; both cases refer to the same (chosen) constant surface gradient $\partial_\theta \rho(R, \theta; \eta) > 0$ of the solute number density. (Being a constant, this gradient scales out and is absorbed in the velocity scale. Therefore the dimensionless ratio $\mathbf{u}/|\mathbf{u}|$ is independent of it.) Since b enters the problem only via the multiplication of $\partial_\theta \rho(R, \theta; t, \eta)$ [see Eq. (B21)], also the absolute value of b drops out from the normalized flow field. The viscosity μ drops out, too. For the unbounded case, the solution [see also Eq. (35) in Ref. 12] is determined from Eqs. (B19a), (B19b), and (B19c) and the requirement that the flow field vanishes at infinity. This implies that in Eq. (B15) all coefficients multiplying terms $\sim r^\ell$ with $\ell \geq 0$ are zero. In the confined case, the flow field is approximated by keeping terms up to $\ell = 50$ [Eqs. (B19)] in the series expansion of Eqs. (B5) and (B9); this provides a reasonably good approximation, except near the boundary at R_1 and for polar angles close to zero or π where apparently there are deviations from the no-slip boundary condition. However, one should keep in mind that in this normalized represen-

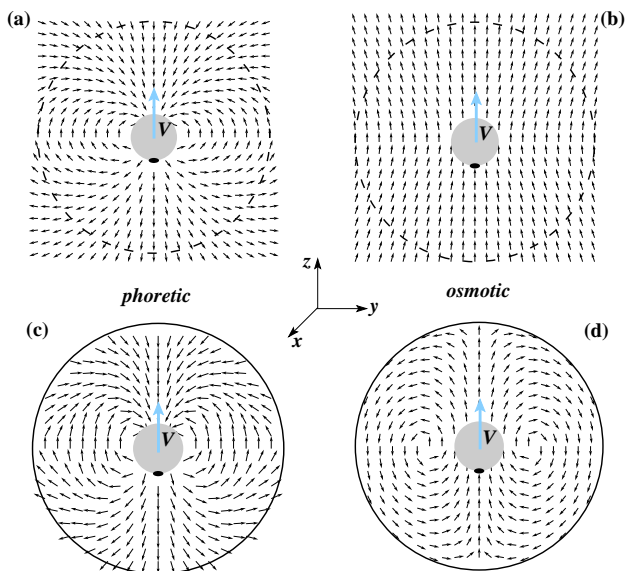


FIG. 4: Normalized velocity fields $\mathbf{u}/|\mathbf{u}|$ in the laboratory frame corresponding to the diffusiphoretic motion due to steric repulsion only ($b < 0$) between the solute and the particle for the case of (a) an unbounded system and (c) a confined system ($\eta = 5$). The panels (b) and (d) show the corresponding results in the case that the motion occurs as a result of a drag provided by the “osmotic pressure” integrated along the surface of the particle. The dashed circles in (a) and (b) indicate the position at which the confining wall is placed in (c) and (d). In all cases (a) - (d) the particle moves upwards, i.e., its velocity \mathbf{V} is in the positive z -direction (as shown by the vector on the particle). Here we consider only time scales on which the movement of the particle does not change the flow fields.

tation of the flow $\mathbf{u}/|\mathbf{u}|$ small numerical deviations from $\mathbf{u} = 0$ at R_1 are sharply overemphasized. For comparison, in Figs. 4(b) and (d) we present the corresponding results for the case in which the motion of the particle occurs as a result of a drag provided by an “osmotic pressure” integrated over the surface of the particle. In this case the particle velocity is oriented along the positive z -direction, too, because of the assumption that the pressure is proportional to the solute number density and thus is larger at the lower hemisphere. In this case Eq. (B19) is solved under the assumption of a no-slip boundary condition at R , i.e., all the coefficients \tilde{k}_ℓ are set to zero; this allows one to obtain a solution in closed form in both the unbounded and the confined cases. Note that in this case p_{-2} is non-zero. It is fixed by the given drag [integrated “osmotic pressure”, Eq. (9)], and thus Eq. (B19), evaluated at $\ell = 1$, leads to a relation between the velocity V and the drag force. (In the unbounded case, this relation is the well-known Stokes formula for the viscous friction on a sphere.) In Eq. (B19a) V sets the velocity scale, which drops out (as well as the drag force, because V is proportional to it) of the dimensionless ratio $\mathbf{u}/|\mathbf{u}|$.

Qualitative differences between these two mechanisms

are particularly clearly visible in the case of the unbounded systems. For example, the flow along the z -axis is in the negative direction (i.e., opposite to the motion of the particle) in the phoretic case, while it is in the positive direction for the “osmotic” propeller; the flow lines for the phoretic motion are closing back and then “slide” along the surface of the particle. Since closed-form analytical expressions are available in these unbounded cases^{12,18}, the qualitative differences noticed above can be correlated with the different characteristics of the flows. In the case of phoretic motion the flow field decays as r^{-3} at large distances r from the particle, which is a “multipole” far-field corresponding to the action of a force-quadrupole disturbance, in contrast to the r^{-1} decay in the osmotic case, which is a “monopole” far-field corresponding to the action of a point-force (“Stokeslet”) disturbance. The faster decay of the velocity field in the first case means that a boundary at R_1 will perturb the phoretic flow much less. This explains why for the phoretic motion the viscous friction increases with the confinement weaker than what would be expected from naively using a Stokes-friction concept.

The flow fields remain qualitatively different even in the presence of the confinement (in particular with respect to the opposite direction of flow along the z -axis), although the differences are not as pronounced as in the unbounded case. A further qualitative difference between the two confined flows is that in (d) a vortex structure is formed fully detached from the particle whereas in (c) the vortex involves flow along the surface of the particle. Due to the presence of the boundary at R_1 , all the terms $\sim r^\ell$ in the expansions of Eq. (B15) are present in the solution and an analysis of the flow in terms of fundamental solutions, as for the unbounded case, is no longer possible. Note that since $\nabla \times \mathbf{u}_{hom} = \nabla \Upsilon$ and $\Upsilon = 0$ [see the text following Eqs. (B7) and (B19f)] one has $\nabla \times \mathbf{u} = \nabla \times \mathbf{u}_p$ so that with Eqs. (B5) and (B6) one obtains

$$\nabla \times \mathbf{u} = \frac{1}{\mu} \mathbf{e}_\phi \sum_{\ell \in \mathbb{Z}} \frac{\tilde{p}_\ell}{\ell + 1} \frac{\partial K_\ell(r, \theta)}{\partial \theta}, \quad (\text{B22})$$

which is in general nonzero [e.g., for “osmotic” flow $\tilde{p}_{-2} \neq 0$ (Eq. (9))]. Thus in agreement with Fig. 4 the flow field can contain vortices.

APPENDIX C: CALCULATION OF THE NUMBER DENSITY OF PRODUCT MOLECULES

Equation (12), subject of the IC and BC conditions given in Eq. (13) is solved by using the Laplace transform and the inversion theorem²⁶:

$$\bar{f}(\zeta) \equiv \mathcal{L}[f] = \int_0^\infty dt e^{-\zeta t} f(t) \quad (\text{C1})$$

and

$$f(t) \equiv \mathcal{L}^{-1}[\bar{f}(\zeta)] := \frac{1}{2\pi i} \int_{\gamma-i\infty}^{\gamma+i\infty} d\zeta e^{\zeta t} \bar{f}(\zeta), \quad (\text{C2})$$

respectively, where $\bar{f}(\zeta)$ (the Laplace transformed quantities are indicated by an overbar) is assumed to be well-defined for $\zeta \in \mathbb{R}^+$ and $\gamma \in \mathbb{R}$ is sufficiently large such that all singularities of $\bar{f}(\zeta)$ lie to the left of the integration path. By taking the Laplace transform of Eqs. (12) and (13) and by using the IC condition of zero number density of the product molecules, one finds that the Laplace transformed density is given by

$$\bar{\rho}(\mathbf{r}, \zeta) = -\bar{a}(\zeta) \bar{G}(\mathbf{r}, q), \quad (\text{C3})$$

where $\bar{a}(\zeta) = \bar{B}(\zeta)/D$ and $\bar{G}(\mathbf{r}, q)$ is the Green's function for the Helmholtz operator $\nabla^2 - q^2$, $q = \sqrt{\zeta/D} > 0$, satisfying the BCs of vanishing normal derivative at $|\mathbf{r}| = R, R_1$.

Decomposing $\bar{G}(\mathbf{r}, q)$ as $\bar{G}(\mathbf{r}, q) = G_s(\mathbf{r}, q; \mathbf{r}_s) + g(\mathbf{r}, q)$, where the singular part G_s is the free space Green's function for the Helmholtz operator (which is known in any spatial dimension d , see, e.g., Ref. 28), the initial problem is reduced to that of finding the solution g of the homogeneous Helmholtz equation subject to the boundary conditions

$$\left(\frac{\partial g(\mathbf{r}, q)}{\partial r} \right) \Big|_{|\mathbf{r}|=R, R_1} = - \left(\frac{\partial G_s(\mathbf{r}, q; \mathbf{r}_s)}{\partial r} \right) \Big|_{|\mathbf{r}|=R, R_1}. \quad (\text{C4})$$

In 3d the singular part of the Green's function is given by²⁸

$$G_s(\mathbf{r}, q; \mathbf{r}_s) = -\frac{q}{4\pi} \frac{e^{-q|\mathbf{r}-\mathbf{r}_s|}}{q|\mathbf{r}-\mathbf{r}_s|}, \quad (\text{C5})$$

while the regular part (i.e., the general solution of the homogeneous Helmholtz equation) can be written as

$$g(r, \theta, q) = \sum_{\ell \geq 0} [\alpha_\ell i_{\ell+1/2}(qr) + \beta_\ell k_{\ell+1/2}(qr)] P_\ell(\cos \theta), \quad (\text{C6})$$

where $i_{\ell+1/2}(z) = \sqrt{\pi/(2z)} I_{\ell+1/2}(z)$ and $k_{\ell+1/2}(z) = \sqrt{\pi/(2z)} K_{\ell+1/2}(z)$ are the modified spherical Bessel functions of the first and third kind, respectively²⁵, P_ℓ is the Legendre polynomial of degree ℓ , while the coefficients α_ℓ and β_ℓ will be fixed to fulfill the boundary conditions.

Using one of the addition theorems for the Bessel functions²⁶ and noting that the angle between \mathbf{r} and \mathbf{r}_s is $\pi - \theta$ (see Fig. 1), G_s can be re-written as

$$G_s(\mathbf{r}, q; \mathbf{r}_s) = - \sum_{\ell \geq 0} c_\ell(q) i_{\ell+1/2}(qr_{<}) k_{\ell+1/2}(qr_{>}) P_\ell(\cos \theta) \quad (\text{C7})$$

where $c_\ell(q) = (-1)^\ell (2\ell + 1)q/(2\pi^2)$, $r_{<} = \min(r, r_s)$, and $r_{>} = \max(r, r_s)$. By combining Eqs. (C6, C7) and the boundary conditions [Eq. (C4)], by noting that $r_s = R + \epsilon$, $\epsilon \searrow 0$ (i.e., the source of particles is on the surface of the particle), and by re-writing the coefficients as $\alpha_\ell \equiv c_\ell i_{\ell+1/2}(qR) \tilde{\alpha}_\ell$ and $\beta_\ell \equiv c_\ell i_{\ell+1/2}(qR) \tilde{\beta}_\ell$, the dimensionless coefficients $\tilde{\alpha}_\ell(qR)$ and $\tilde{\beta}_\ell(qR)$ are determined by the solution of the following closed system of two linear equations with two unknowns ($\tilde{\alpha}_\ell$ and $\tilde{\beta}_\ell$):

$$\tilde{\alpha}_\ell + \tilde{\beta}_\ell w_{\ell+1/2}(qR) = v_{\ell+1/2}(qR), \quad (\text{C8a})$$

$$\tilde{\alpha}_\ell + \tilde{\beta}_\ell w_{\ell+1/2}(\eta qR) = w_{\ell+1/2}(\eta qR), \quad (\text{C8b})$$

where $v_{\ell+1/2}(z) := k_{\ell+1/2}(z)/i_{\ell+1/2}(z)$ and $w_{\ell+1/2}(z) := [dk_{\ell+1/2}(z)/dz]/[di_{\ell+1/2}(z)/dz]$. The solution $\tilde{\alpha}_\ell$ and $\tilde{\beta}_\ell$ acquires a dependence on η via Eq. (C8b): $\hat{\alpha}_\ell = \hat{\alpha}_\ell(qR, \eta)$ and $\hat{\beta}_\ell = \hat{\beta}_\ell(qR, \eta)$, with $qR = R\sqrt{\zeta/D}$. This determines the Green's function $\bar{G}(\mathbf{r}, q)$ and thus the Laplace transformed density $\bar{\rho}(\mathbf{r}, \zeta)$ [Eq. (C3)] from which, in principle, the density $\bar{\rho}(\mathbf{r}, t)$ is obtained via the inverse Laplace transformation. Note that although the final result is in the form of a series, the quantities in which we are interested, in particular the phoretic velocity $V(t)$ [Eq. 10], involve integrals over the polar angle θ of the product between this series and a specific ℓ Legendre polynomial $P_\ell(\cos \theta)$ [$\ell = 1$ in the case of the velocity, $\ell = 0$ in the case of the total number of product molecules (see below)] and thus only one of the terms from the series will contribute.

We make the following three remarks:

- (i) Since for $qR > 0$ one has $\lim_{\eta \rightarrow \infty} w_{\ell+1/2}(\eta qR) = 0$, in the limit $\eta \rightarrow \infty$ one finds $\tilde{\alpha}_\ell = 0$ and Eq. (C8a) reduces to the corresponding BC in Ref. 5, i.e., as expected the solution for the unbounded case is recovered.
- (ii) Equations (C8a) and (C8b) will not coincide in the limit $\eta \rightarrow 1$ because even in this limit of extreme confinement a source singularity is present at r_s and is picked up by $G_s(q)$ [Eq. (C7)].
- (iii) The Laplace transform $\bar{N}(p)$ of the total number of product particles in the system at time t is

$$\begin{aligned} \bar{N}(p = Dq^2) &= 2\pi \int_R^{R_1} dr r^2 \int_0^\pi d\theta \sin \theta P_0(\cos \theta) [-\bar{a}(p)] \bar{G}(q) \\ &= -4\pi \bar{a}(p) c_0(q) i_{1/2}(qR) \\ &\quad \times \int_R^{R_1} dr r^2 [\tilde{\alpha}_0 i_{1/2}(qr) + (\tilde{\beta}_0 - 1) k_{1/2}(qr)] \\ &= D\bar{a}(p)/p \Rightarrow N(t) = \int_0^t dt' A(t'), \end{aligned} \quad (\text{C9})$$

i.e., as expected $N(t)$ is given by the time integral of the production rate, providing a welcome consistency check.

-
- * Electronic address: Mihail.Popescu@unisa.edu.au; also at: Max-Planck-Institut für Metallforschung, Heisenbergstr. 3, 70569 Stuttgart, Germany
- † Electronic address: dietrich@mf.mpg.de
- ‡ Electronic address: oshanin@lptl.jussieu.fr; also at: Max-Planck-Institut für Metallforschung, Heisenbergstr. 3, 70569 Stuttgart, Germany
- ¹ W.F. Paxton, A. Sen, and T.E. Mallouk, Chem.–Eur. J. **11**, 6462 (2005).
 - ² W.F. Paxton, S. Sundararajan, T.E. Mallouk, and A. Sen, Angew. Chem., Int. Ed. **45**, 5420 (2006); W.F. Paxton, K.C. Kistler, C.C. Olmeda, A. Sen, S.K.St. Angelo, Y. Cao, T.E. Mallouk, P.E. Lammert, and V.H. Crespi, J. Am. Chem. Soc. **126**, 13424 (2004).
 - ³ R.F. Ismagilov, A. Schwartz, N. Bowden, and G.M. Whitesides, Angew. Chem., Int. Ed. **41**, 652 (2002).
 - ⁴ J.M. Catchmark, S. Subramanian, and A. Sen, Small **1**, 1 (2005).
 - ⁵ R. Golestanian, T.B. Liverpool, and A. Ajdari, Phys. Rev. Lett. **94**, 220801 (2005).
 - ⁶ J.R. Howse, R.A.L. Jones, A.J. Ryan, T. Gough, R. Vafabakhsh, and R. Golestanian, Phys. Rev. Lett. **99**, 048102 (2007).
 - ⁷ G. Rückner and R. Kapral, Phys. Rev. Lett. **98**, 150603 (2007).
 - ⁸ R. Golestanian, T.B. Liverpool, and A. Ajdari, New J. Phys. **9**, 126 (2007).
 - ⁹ F. Peruani and L.G. Morelli, Phys. Rev. Lett. **99**, 010602 (2007).
 - ¹⁰ P.G. Saffman and M. Delbrück, Proc. Nat. Acad. Sci. USA **72**, 3111 (1975); P.G. Saffman, J. Fluid Mech. **73**, 593 (1976).
 - ¹¹ C. Barentin, C. Ybert, J.-M. di Meglio, and J.-F. Joanny, J. Fluid Mech. **397**, 331 (1999); C. Barentin, P. Muller, C. Ybert, J.-F. Joanny, and J.-M. di Meglio, Eur. Phys. J. E **2**, 153 (2000).
 - ¹² J.L. Anderson, Ann. Rev. Fluid Mech. **21**, 61 (1989).
 - ¹³ M.K. Phibbs and P.A. Giguère, Can. J. Chem. **29**, 173 (1951).
 - ¹⁴ A. Einstein, “On the Movement of Small Particles Suspended in a Stationary Liquid Demanded by the Molecular-Kinetic Theory of Heat” in *Investigations on the theory of the Brownian motion*, Ed. R. Fürth, transl. by A. D. Cowper (Dover, New York, 1956).
 - ¹⁵ F. Juelicher and J. Prost, arXiv:0812.2924v1 (2008).
 - ¹⁶ S.R. de Groot and P. Mazur, *Non-Equilibrium Thermodynamics* (North-Holland, Amsterdam, 1962), Ch. V.2, p. 44.
 - ¹⁷ A. Ajdari and L. Bocquet, Phys. Rev. Lett. **96**, 186102 (2006).
 - ¹⁸ J. Happel and H. Brenner, *Low Reynolds number hydrodynamics* (Noordhoff International, Leyden, 1973), Ch. 3-2, pp. 62-67.
 - ¹⁹ H. Lamb, *Hydrodynamics* (Dover, New York, 1945), p. 594.
 - ²⁰ A.L. Zydney, J. Colloid Interface Sci. **169**, 476 (1995).
 - ²¹ F.A. Morrison Jr., J. Colloid Interface Sci. **34**, 210 (1970).
 - ²² U.M. Córdoba-Figueroa and J.F. Brady, Phys. Rev. Lett. **100**, 158303 (2008).
 - ²³ N. Bala Saidulu and K. L. Sebastian, J. Chem. Phys. **128**, 074708 (2008).
 - ²⁴ A.T. Chwang and T.Y.-T. Wu, J. Fluid Mech. **67**, 787 (1975).
 - ²⁵ M. Abramowitz and I.A. Stegun, *Handbook of Mathematical Functions with Formulas, Graphs, and Mathematical Tables* (Dover, New York, 1965) pp. 374, 443.
 - ²⁶ H.S. Carslaw and J.C. Jaeger, *Conduction of Heat in Solids* (University Press, Oxford, 1959), pp. 377, 381.
 - ²⁷ P. Tierno, R. Golestanian, I. Pagonabarraga, and F. Sagués, Phys. Rev. Lett. **101**, 218304 (2008).
 - ²⁸ S. Hassani, *Mathematical Physics: A Modern Introduction to Its Foundations* (Springer, New York, 1998) p. 631.